

the viral gp120 envelope glycoprotein, and interrupting virus attachment to the negatively charged heparan sulfate proteoglycans on cell surface, and inhibiting the specific binding to the CD4 receptor of CD4⁺ cells. Some of these compounds can also interfere with later events in receptor-mediated fusion by virtue of attachment to gp120. These compounds probably do not penetrate into cells because of their mass and highly anionic charge, but rather, act as antiviral agents by impeding the attachment and subsequent entry of virus particles into the cell.

A number of sulfated polysaccharides, including dextran sulfate and heparin, have been reported to have potential as antiviral drugs, since they inhibit the replication of a variety of viruses in vitro (Baba et al., 1988; Bartolini et al., 2003; Nakashima et al., 1989; Ylisastigui et al., 2000). The extent of inhibition appeared to be dependent on both the viral strain and host cell type. Dextran sulfate interferes with the association of gp120 with CXCR4 while having no detectable effect on gp120-CD4. The interaction between polyanions and X4 or X4R5 gp120 was readily detectable, whereas weak or undetectable binding was observed with R5 gp120 (Moulard et al., 2000). Cosalanes inhibited the binding of gp120 to CD4 as well as the fusion of the viral envelope with the cell membrane and is more potent against R5 HIV-1 RF in CEM-SS cells than against vs X4 HIV-1 IIIB in MT-4 cells (Santhosh et al., 2001).

Polygonum tinctorium has been used extensively in Chinese and Japanese folk medicine for the treatment of many infectious diseases and is believed to have effects such as detoxification, anti-pyrexia and anti-nociception. Extracted constituents of this medicinal plant, such as tryptanthrin, has been shown to possess anti-fungal, cancer chemopreventive and anti-bacterial activities (Honda and Tabata, 1979; Koyama et al., 2001; Kataoka et al., 2001; Miyake et al., 2003), while pigment (PtP) has an anti-anaphylactic activity (Kim et al., 1998). In this study, we report for the first time the potent anti-HIV-1 and HSV-1 activity of an aqueous extract from the fermented leaves of *Polygonum tinctorium* (*Sukumo*). This extract was found to be highly selective against HIV-1 and HSV-1 in vitro. *Sukumo* extract suppresses production of HIV-1 by inhibiting the viral entry process through binding to the virus envelope and thus preventing HIV-induced syncytium formation with an exceedingly broad therapeutic window. Based on the results of physico-chemical analysis of the anti-viral active factor, it is putatively a novel polyanionic high-molecular-weight compound containing a phenolic substructure in aqueous extract of *Sukumo*.

2. Materials and method

2.1. Compound

Sukumo was collected from the leaves of *Polygonum tinctorium* (Tokushima, Japan) and fermented for 3 months, which was provided and identified by Dr. Matsuda. Voucher

specimens were deposited at the Institute of Hemorheological Function of Food Co. Ltd., Hyogo, Japan. *Sukumo* powder (100 g) was refluxed three times with 99.9% ethanol, then with water (1 l). The aqueous solution was clarified by filtering through a 0.2 µm filter. The high-molecular compounds were precipitated from the aqueous extracts of *Sukumo* by 66.6% ethanol, which were collected by centrifugation (10,000 rpm, 30 min) in a yield of 26.8% (26.8 g). Anti-HIV activity of the *Sukumo* extract was tested and stored at 4 °C before use.

2.2. Cells and virus

MT-4, Molt-4 cells and Molt-4 cells chronically infected with the HIV-1 (III_B) strain (Molt-4/IIIB) were cultured in RPMI-1640 medium supplemented with 10% fetal bovine serum (FBS) (Cansera International Inc., Canada) and antibiotics (100 µg/ml penicillin/100 µg/ml streptomycin). 293T, Vero and stably expressing CD4-CCR5 of Hos cells were maintained in Dulbecco's Modified Eagle's medium (DMEM) containing the same supplements. X4/HIV-1 (III_B) was prepared by propagation in Molt-4/IIIB cells. HIV-1 molecular clones of the X4 HIV-1 strain NL4-3 and the R5 HIV-1 strain JRCSF were prepared by transfection of 293T cells with NL4-3 or JRCSF plasmids carrying full-length proviral DNA. The culture supernatants were clarified by 0.45 µm filters and frozen at -80 °C. Herpes simplex virus type 1 was propagated in Vero cells (kindly provided by Dr. Shaku). Cell-free virus stock was prepared by sonication of HSV-infected Vero cells in 9% skim milk and stored at -80 °C until use.

2.3. Antiviral assay

To determine the anti-HIV-1 activity and cytotoxicity of the *Sukumo* extract, MT-4 cells were either infected with HIV-1 (III_B) strains at a multiplicity of infection (MOI) of 0.01 or un-infected (mock infection). Cell viability was quantified with MTT (Dojindo, Kumamoto, Japan) assay for MT-4 cells. EC₅₀ values were calculated in infected cells for the anti-HIV-1 effect and CC₅₀ values were calculated in un-infected cells for drug cytotoxicity (Ichiyama et al., 2003). Peripheral blood mononuclear cells (PBMCs) from HIV-1-seronegative donors were isolated by Ficoll-Hypaque density gradient centrifugation. PHA (1 µg/ml, Sigma-Aldrich)/IL-2 (100 U/ml, Shionogi, Osaka, Japan) activated PBMCs were infected for 2 h with 20 ng of HIV-1 p24 Gag (X4/NL4-3 or R5/JRCSF) in the presence or absence of the *Sukumo* extract (0.64–400 µg/ml), washed three times with PBS and cultured for 7 days in RPMI-1640 medium/10% FBS plus 100 U/ml IL-2 with or without the *Sukumo* extract. HIV-1 p24 Gag of culture supernatant was determined by automated enzyme-linked immunosorbent assay (EILSA) (Fuji Rebio Inc., Tokyo, Japan). In this assay the p24 antigen from Zeptomatrix (Buffalo, New York) was used as the standard. Chronically HIV-1 (III_B)-infected Molt-4 cells were

co-cultured with HIV non-infected Molt-4 cells (ratio = 1:1) at 37 °C for 1 day in the presence of a test compound at graded concentrations. Cell–cell fusion was analyzed by confocal microscopic assessment of syncytium formation.

Sukumo extract were also tested as an inhibitor of HSV-1 replication in Vero cells using a standard plaque assay. Two hour after treatment with *Sukumo* extract, Vero cells were subjected to a 1-h infection with about 50 PFU of HSV-1 in the absence or presence of serially diluted *Sukumo* extract and then cultured with 199 medium supplemented with 1% FBS, human γ -globulins (164 μ g/ml, Sigma-Aldrich) and antibiotics, with or without compounds cultured for 4 days. The cells were stained with Giemsa solution. The numbers of viral plaques were calculated as a percentage of the tested control in order to determine the percent inhibition. The EC₅₀ value is the concentration of compound that inhibits viral replication by 50% relative to control.

2.4. Virus binding and entry assay

Human MT-4 cells (4×10^5) were suspended in fresh medium in the presence or absence of various concentrations of *Sukumo* extract at 37 °C for 1 h. After washing, the cells were incubated with HIV-1 NL4-3 (200 ng of p24 Gag) for 2 h on ice or at 37 °C in the absence or presence of extract. The cells were washed with PBS/2% FBS and the pellet re-suspended with 500 μ l of lysis buffer (PBS containing 5% TritonX-100 and 1% BSA). Levels of p24 Gag were quantified by an automated ELISA system.

2.5. Flow cytometric analysis

MT-4 or Hos/CCR5 cells (5×10^5) were pretreated with normal human IgG (Zymed, South San Francisco) at 0.1 mg/ml in PBS containing 2% FBS buffer for 30 min on ice to block the Fc receptors and then were treated by anti-CXCR4 antibodies (5 μ g/ml, 12G5, R&D Systems Inc.) or anti-CCR5 antibodies (3.5 μ g/ml, 2D7, Biosciences-Pharmingen, San Diego) in the presence or absence of *Sukumo* extract at 37 °C for 2 h. Cells were washed with PBS/2% FBS and strained with FITC-conjugated anti-mouse IgG (0.02 mg/ml, American Qualex) for 30 min on ice. Pretreated MT-4 cells also were stained with FITC-conjugated anti-human CD4 or monoclonal mouse antibodies of isotype IgG (negative control for flow cytometry) (1:50 dilution, DAKO). The cells were fixed in 1% paraformaldehyde-PBS solution and analyzed on FACS Calibur (Becton Dickinson), a flow cytometer with CELLQUEST software (Becton Dickinson).

2.6. Single-cycle infectivity assay

Pseudotyping vesicular stomatitis virus protein G (VSV-G) onto HIV cores from an env-defective reporter virus was carried out as follows. Plasmid DNA (10 μ g) encoding envelope from VSV-G was co-transfected with pNL-E env(–)

nef(–) (20 μ g) into 293T cells using the calcium phosphate method. The virus titer was determined based on the level of p24 Gag. Time course assays were conducted to determine which steps in viral infection (entry and post-entry) were inhibited by *Sukumo* extract. Three treatment schedules were applied for HIV-1 infection with 293T cells, which were infected with pseudotyped HIV-1/VSV-G viruses (5 ng/ml of p24 Gag). The amount of p24 Gag in culture supernatant was determined to assess HIV-1 replication. *Sukumo* extract was used at serial concentrations in a range of 0.16–100 μ g/ml and added at different times. The levels of p24 Gag were determined after 3 days of incubation by an auto-ELISA system.

2.7. *Sukumo* extract binding assay

The binding assay was used to determine the affinity of *Sukumo* extract for virions by viral replication assay. Separation of *Sukumo* extract and virus was carried out on a chromatography of gel filtration system with a column of Sephacryl S-500 (1 by 18 cm) (Amersham Pharmacia Biotech, Sweden). The column was equilibrated and the compounds were eluted from column with PBS. The samples were separated into the following three samples; *Sukumo extract control*: up to 150 μ l of *Sukumo* extract (16 mg/ml), with 450 μ l of RPMI-1640 medium containing 10% FBS added; *virus control*: up to 150 μ l of PBS, with 450 μ l of cultured supernatant containing HIV-1 NL4-3 added; *Sukumo extract–virus mixture*: up to 150 μ l of *Sukumo* extract, with 450 μ l of cultured supernatant containing HIV-1 NL4-3 added. A volume of 500 μ l of each sample was injected onto the analytical column after incubation at 37 °C for 1 h and one fraction of eluant was collected (1 ml) on ice. The elution peak of the *Sukumo* extract control fractions at a wavelength of 492 nm and anti-HIV-1 IIIIB activity by MTT assay were monitored to determine the elution position of *Sukumo* extract (Fig. 4A). The levels of p24 Gag in the eluted fractions were measured with auto-ELISA to determine the elution position of virus (Fig. 4B). Viral infectivity was analyzed for the eluted fractions of the virus control and *Sukumo* extract–virus mixture; the selected fractions 6 and 7 were clarified by 0.2 μ M filter. MT-4 cells (4×10^5 /ml) were infected by a mixture of the eluted fractions. Two hours after infection, the cells were washed and added to fresh RPMI-1640/10% FBS medium, cultured for 4 days and the p24 Gag of supernatant was measured.

2.8. Separation of compound

Anion exchange chromatography was carried out on a DEAE-Sephacel column, which had been equilibrated with phosphate buffer (pH 7.2). The bound sample was eluted by stepwise increases of the NaCl concentrations in phosphate buffer. The eluted fractions were analyzed for anti-HIV activity using the MTT assay method. The *Sukumo* extract was also separated with 15% SDS-PAGE. The gel was stained

by silver reagent and cut as described in Fig. 6B. *Sukumo* was re-extracted with RPMI-1640 medium from the SDS-gel fractions and collected supernatants for anti-HIV-1 activity.

3. Results

3.1. Spectrum of anti-viral activity of *Sukumo* extract

The anti-HIV-1 activity of *Sukumo* extract was first investigated by conventional MTT assay using MT-4 cells. *Sukumo* extract completely inhibited HIV-1 (III_B strain) replication in MT-4 cells at a concentration as low as 3.9 $\mu\text{g/ml}$. Its 50 and 90% effective concentrations (EC_{50} and EC_{90}) were 0.5494 and 2.1378 $\mu\text{g/ml}$, respectively. The 50% cytotoxic concentration (CC_{50}) was found to be >1000 $\mu\text{g/ml}$ (Fig. 1A), and the selectivity index (ratio of CC_{50} to EC_{50}) of *Sukumo* extract was >1820, indicating that this compounds is very potent and selective.

Sukumo extract was also evaluated for the inhibition of wild-type herpes simplex virus-1 replication in infected Vero cells, using a standard viral plaque assay (Fig. 1B). *Sukumo* extract, and exhibited anti-viral activity with an EC_{50} value of 11.56 $\mu\text{g/ml}$. However, no inhibitory activity was observed against influenza A virus, poliovirus and SARS virus when *Sukumo* extract was tested at concentrations ranging from 3.2 to 400 $\mu\text{g/ml}$ (data not shown).

3.2. Anti-HIV-1 activity of *Sukumo* extract

Sukumo extract inhibited a variety of HIV-1 isolates, including a laboratory adapted isolate III_B strain, laboratory molecular clones X4 type NL4-3 and R5 type JRCSF in a variety of cells, including Molt-4, Jurkat, PM1, and CD4-CCR5 expressing Hos cells (data not shown). The inhibitory activity of *Sukumo* extract against X4 HIV-1 (NL4-3) and R5 HIV-1 (JRCSF) replication in PBMCs was also demonstrated

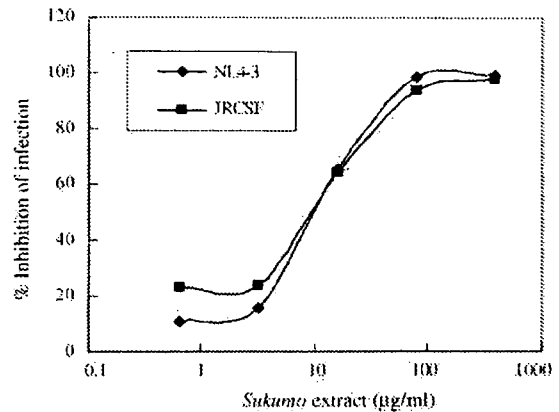


Fig. 2. Anti-HIV-1 activity of *Sukumo* extract in PHA-stimulated PBMCs. PHA-stimulated PBMCs were infected for 2 h at 37 °C in the absence or presence of 0.64–400 $\mu\text{g/ml}$ *Sukumo* extract followed by washing. 1×10^6 /ml infected cells per well were seeded in 24-well plate and were incubated for 7 days in the absence or presence of appropriate concentrations of compound. Quantity of HIV-1 p24 Gag was measured by auto-ELISA system.

by p24 assay of culture supernatants of the cells infected with the viruses exhibiting EC_{50} values of 12.02 and 11.5 $\mu\text{g/ml}$, respectively (Fig. 2). The p24 Gag levels of untreated samples of HIV-1 NL4-3 and JRCSF were 27.914 and 14.096 ng/ml, respectively. HIV-1 replication in MT-4 cells appeared to be more sensitive to *Sukumo* extract than in PBMCs.

3.3. Inhibition of HIV-1 binding and entry to the cells

In the various steps of the HIV-1 life cycle, we next investigated at which step *Sukumo* extract exerts its effect as an HIV-1 antagonist. To determine whether the viral binding to cells is a target of *Sukumo* extract, a binding assay was carried out to measure the effect of *Sukumo* extract on virions/cell surface interactions. MT-4 cells were mixed with X4 virus NL4-3 on ice for 2 h, and then the cells washed to remove the unbound viruses. The results demonstrate that

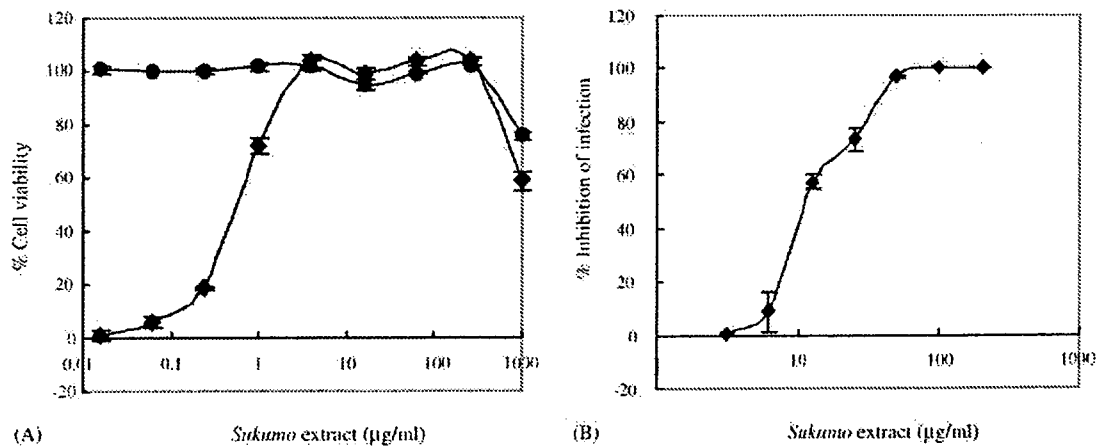


Fig. 1. Anti-viral activity of *Sukumo* extract. (A) Anti-HIV-1 activity of *Sukumo* extract in MT-4 cells was measured by MTT assay. HIV-1 (III_B) was used in this study (●● mock infected and ♦♦ HIV-1) and the EC_{50} values for inhibition of *Sukumo* extract against HIV-1 replication were determined. (B) Anti-HSV-1 activity of *Sukumo* extract in Vero cells was determined by plaque assay. The results shown are mean \pm S.D. of triplicates.

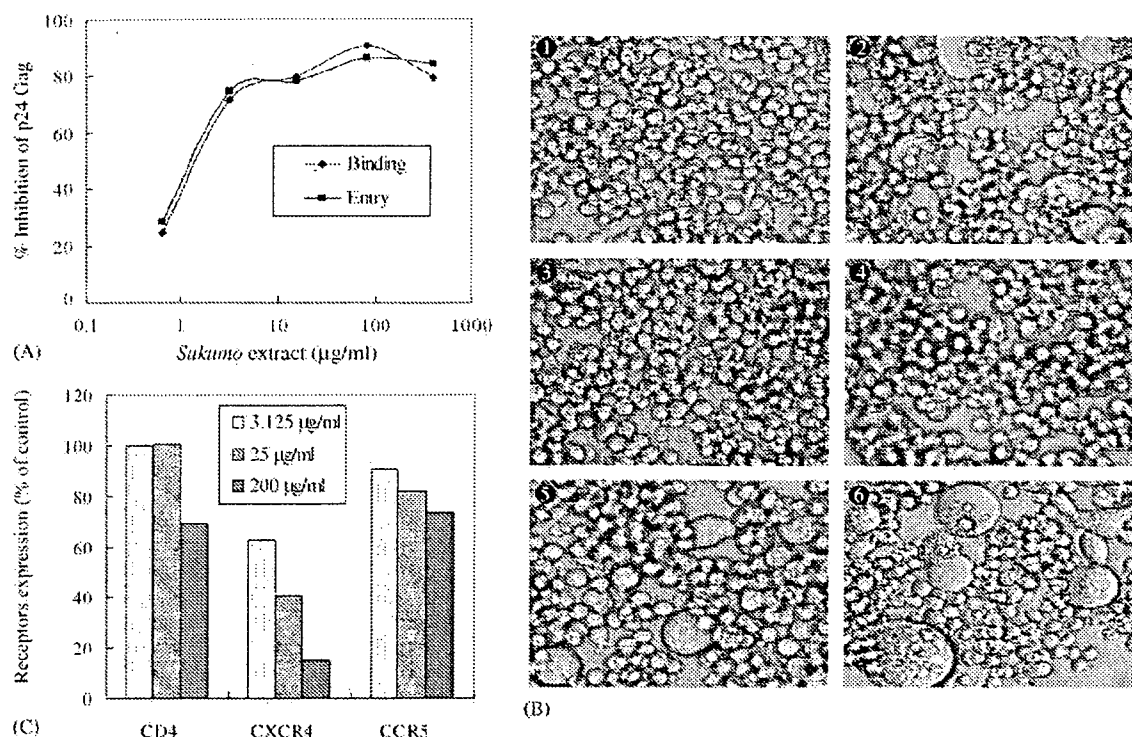


Fig. 3. Inhibition of HIV-1 entry and syncytia formation by *Sukumo* extract. (A) Inhibition of HIV-1 binding and entry into MT-4 cells by *Sukumo* extract. The cells were incubated for 2 h on ice or 37 °C with HIV-1 NL4-3 strain in the presence of various concentrations (0.64–200 µg/ml) of *Sukumo* extract. The levels of p24 antigen of virions bound to or entered in MT-4 cells were measured in the presence of different concentrations of *Sukumo* extract. The percentage of inhibition of virus binding or entry was defined as $[1 - (\text{p24 Gag with } Sukumo / \text{p24 Gag without } Sukumo \text{ extract})] \times 100\%$. (B) Inhibition of cell–cell fusion by *Sukumo* extract. (1) Molt-4 cells; (2) Molt-4 and Molt-4/IIIIB cells co-culture; (3) 200 µg/ml *Sukumo* extract; (4) 25 µg/ml *Sukumo* extract; (5) 3.125 µg/ml *Sukumo* extract and (6) 0.39 µg/ml *Sukumo* extract. (C) Down-modulation of CD4, CXCR4 and CCR5 expression in MT-4 or CCR5 expressing Hos cells after treatment with *Sukumo* extract. Cells were exposed to an anti-CD4, anti-CXCR4 (12G5) or anti-CCR5 (2D7) antibody in the presence of 3.125, 25 and 200 µg/ml *Sukumo* extract, or to a negative control antibody, followed by labeling with a FITC-conjugated anti-mouse Ig probe and analyzed by flow cytometry. These results are representative of multiple experiments and microscopic fields.

Sukumo extract blocked virus–cell binding with an EC_{50} of 2.02 µg/ml (Fig. 3A). The inhibitory effect of *Sukumo* extract on HIV-1 entry to cells was also studied in MT-4 cells. Cells were incubated with the same virus at 37 °C for 2 h, treated with trypsin to remove bound virions, and then the intracellular p24 Gag of HIV-1 was measured. *Sukumo* extract inhibited viral entry with an EC_{50} of 1.84 µg/ml (Fig. 3A). The binding and entry of HIV-1 NL4-3 in MT-4 cells was efficiently inhibited by *Sukumo* extract in a dose-dependent manner. A similar result was also observed with R5 type HIV-1 JRCSF on Hos/CD4-CCR5 cells (data not shown). These experiments show that there is a good correlation between the anti-HIV activity and the inhibitory activity against virus binding/entry induced by the *Sukumo* extract.

Sukumo extract also completely prevented syncytium formation through co-culture of Molt-4 and HIV-1-converted Molt-4 cells at a concentration of 25 µg/ml and efficiently prevented it even at 3.125 µg/ml (Fig. 3B). These data indicate that *Sukumo* extract exerted its effect at an initial step of HIV-1 infection, such as viral entry and membrane fusion in the target cells.

We then analyzed changes in CD4 and CXCR4 expression on MT-4 cells and CCR5 expression on Hos/CD4-CCR5 cells upon treatment with different concentrations of *Sukumo* extract. Only a high concentration of *Sukumo* extract (200 µg/ml) caused down-expression of CD4 (68.87% of control). When *Sukumo* extract was used at the concentrations of 200, 25 and 3.125 µg/ml, the levels of CXCR4 expressed were only 15.33, 40.64 and 62.81% of control, respectively. In contrast, the levels of CCR5 expression on the surface of Hos cells were 73.25, 82.01 and 90.6% of control at the same concentration range (Fig. 3C).

3.4. Interaction of *Sukumo* extract with the HIV-1 envelope

To determine the *Sukumo* extract and HIV-1 interaction, we applied a chromatographical analysis using a Sephacryl S-500 for separation of the virus particles and the *Sukumo* extract based on differential molecular size. When *Sukumo* extract was fractionated, the main anti-HIV-1 activity was eluted in fractions 10–14, as revealed by the MTT assay

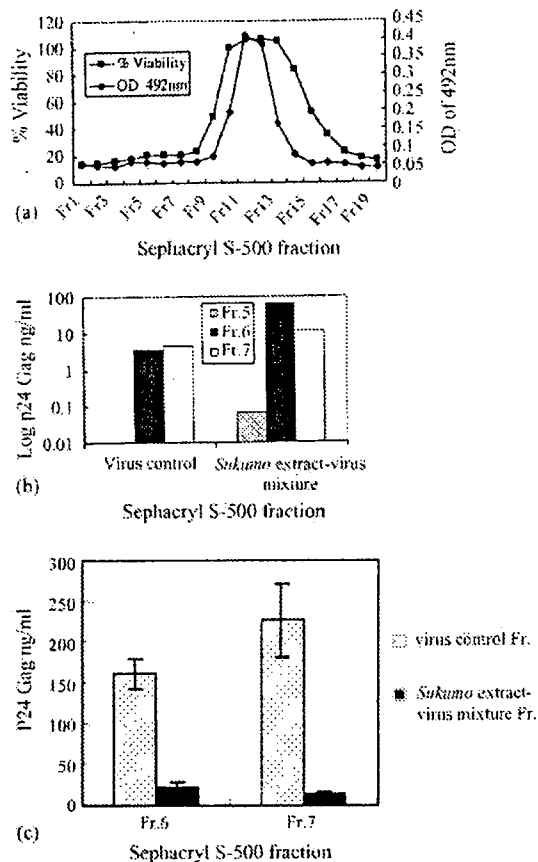


Fig. 4. Specific binding of *Sukumo* extract to HIV-1 virions, resulting in viral entry blockade and inhibition of HIV-1 replication in MT-4 cells. Experiments were carried out with a Sephacryl S-500 column in which three samples of *Sukumo* extract control, virus control (HIV NL4-3) and *Sukumo* extract–virus mixture were separated with a chromatograph column, respectively. (A) Anti-HIV-1 activity and absorbance of the wavelength of 492 nm from chromatogram fractions of *Sukumo* extract control eluate. Absorbance of *Sukumo* extract control fractions was measured at the wavelength of 492 nm (◆); the activity of each fraction was tested against HIV-1 replication by MTT assay, and then the viability of cells was calculated (■). (B) The quantity of HIV-1 p24 Gag was measured by auto-ELISA p24 Gag assay from chromatogram fractions 5–7 of virus control eluate and *Sukumo* extract–virus mixture eluate. (C) Infectivity of HIV-1 NL4-3 from chromatogram fractions of the virus control and *Sukumo* extract–virus mixture. The eluted fractions 6 and 7 were selected and infected into MT-4 cells for 2 h at 37 °C. After washing, the cells were incubated for 4 days and p24 Gag of culture supernatant was measured by auto-ELISA.

(Fig. 4A). On the other hand, HIV-1 was eluted in fractions 6 and 7 as shown by p24 assay (Fig. 4B left). When an excess amount of *Sukumo* extract was mixed with HIV-1 and separated with Sephacryl, the viral peak was detected in fractions 6 and 7 once again (Fig. 4B right), while anti-HIV activity was still observed in fraction 10–14 (data not shown). To see whether these fractions contained an infective capacity of HIV-1, the amount of p24 Gag was assessed in the supernatant of MT-4 cells after infection. We used the same volume (150 μ l) of eluted fractions 6 and 7 from viral control, which contained 0.53 and 0.69 ng of p24 antigen, or those

from the *Sukumo* extract–virus mixture which contained 10.24 and 1.78 ng of p24 antigen to infect 4×10^5 MT-4 cells, respectively. As shown in Fig. 4C, fractions 6 and 7 obtained from the viral control exhibited high HIV-1 activity (161.35 and 226.32 ng/ml in p24 level) 4 days after infection while fractions 6 and 7 from the *Sukumo* extract–virus mixture had p24 levels as low as 21.6 and 13.76 ng/ml, respectively. These results strongly suggests that the *Sukumo* extract specifically bound to viral particles and was efficiently trapped by viral particles so that viral infectivity was significantly abrogated due to the blockage of entry into the cells.

3.5. Effect of *Sukumo* extract on VSV-G pseudotyped HIV-1 replication

Although all the data provided evidence that HIV-1 entry could be a primary anti-viral target of *Sukumo* extract, there still remained the possibility that *Sukumo* extract exerts its effect on a late step of viral replication. To address this, a time course assay was performed using a single cycle infection with VSV-G pseudotyped HIV-1 and 293T cells. P24 Gag in the supernatant was measured 3 days post-infection. The result showed that a dose-dependent anti-viral activity of *Sukumo* extract was observed when it was added at the time B (entry) step. In contrast, the inhibition was not seen when *Sukumo* extract was added at the time A (pre-treatment) or time C step (post-entry) at any concentrations studied (range 0.16–100 μ g/ml) (Fig. 5). A similar result was also observed when Hos/CD4-CCR5 cells were used (data not shown). These results suggest that *Sukumo* extract does affect an early step, not a post-entry step, of the viral life cycle.

Based on these studies, we conclude that there is persuasive evidence that *Sukumo* extract is a binding inhibitor that interferes with virion/cells interactions and that this inhibition is likely mediated through binding to the HIV-1 viral envelope.

3.6. Physico-chemical characterization of anti-viral factors in *Sukumo* extract

The anti-viral factor was extracted from *Sukumo* using organic solvent and water. Inhibitory activity was found in the aqueous extract. Crude *Sukumo* extract was fractionated by DEAE-Sephacel column chromatography. The main fractions which had anti-viral activity was eluted from the column by 1.0–2.0 M NaCl (Fig. 6A). The *Sukumo* extract was also separated by using SDS-PAGE and anti-HIV-1 activity was detected in fractions 3–7 of the SDS-gel extracts corresponding to a molecular weight of 10,000–50,000 (Fig. 6B). Gas chromatography analysis of the acid hydrolysates of the *Sukumo* extract revealed the carbohydrate contents of Ara:Xyl:Man:Gal:Glc were 5.1:1:2.1:3.3:2.6 (Table 1) and SDS-PAGE/PAS staining yielded a bright red band (Zacharius et al., 1969) (data not shown). Elemental analysis revealed that the sulfur content is 1.14% in the

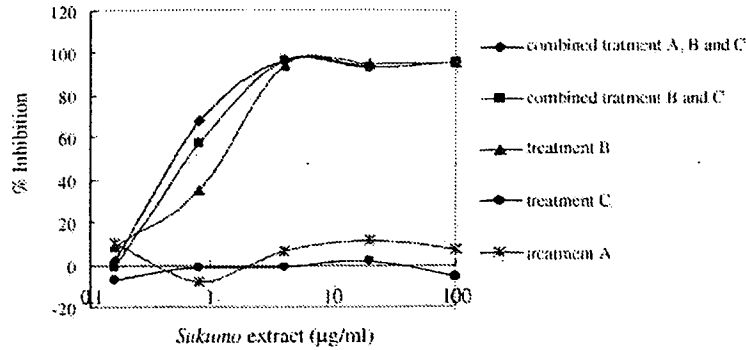
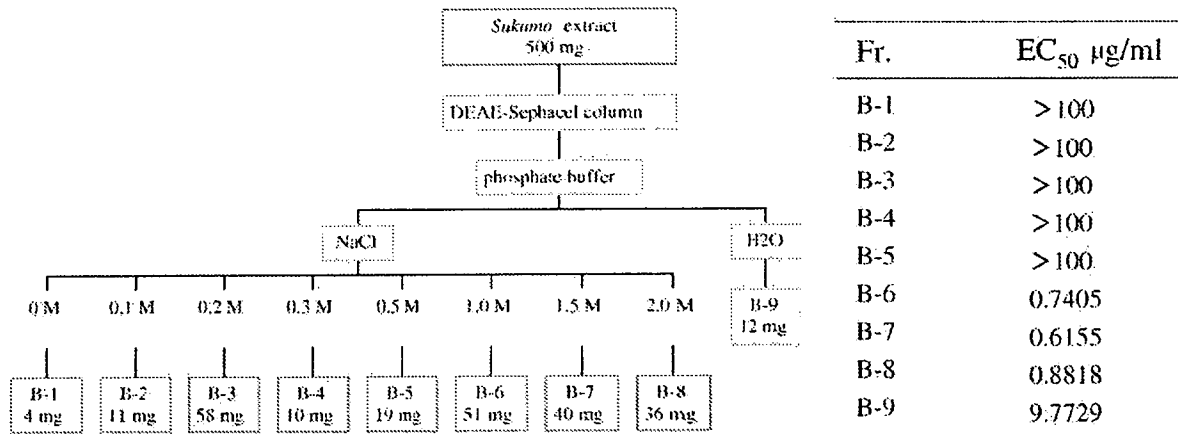
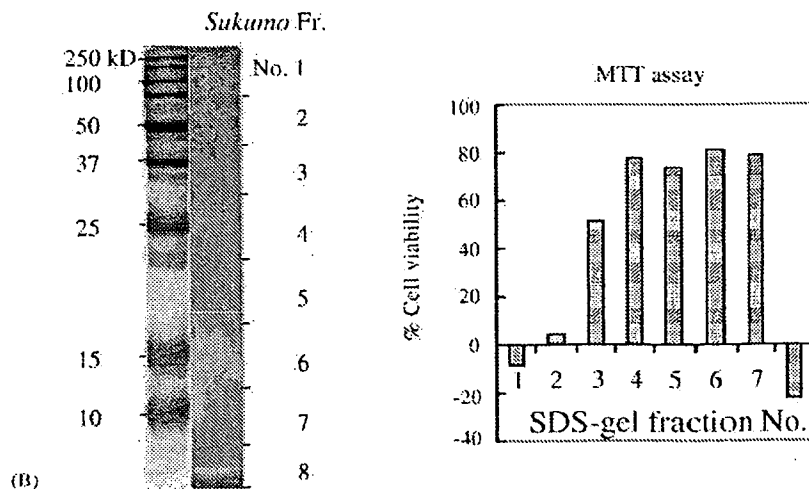


Fig. 5. Effect of *Sukumo* extract on VSV-G pseudotyped HIV-1 replication. 293T cells were infected with the HIV-1 NL-E strain lacking env and nef with VSV-G envelope of pseudotyped virus. 0.16–100 µg/ml *Sukumo* extract was used and anti-HIV-1 activity was determined 3 days later by measuring p24 Gag. Treatment A (a pre-entry step): the cells were incubated with *Sukumo* extract for 2 h at 37°C and washed before exposure to virus, and then the cells were infected and incubated in the absence of *Sukumo* extract. Treatment B (an entry step): the cells were exposed to virus in the presence of *Sukumo* extract for 2 h, then both *Sukumo* extract and unabsorbed viruses were removed by washing. The cells were further incubated in the absence of *Sukumo* extract. Treatment C (a post-entry step): the cells were infected with virus for 2 h, unabsorbed virus were removed and further incubated in presence of *Sukumo* extract.



(A)



(B)

Fig. 6. Physico-chemical characterization of *Sukumo* extract. (A) *Sukumo* extract was analyzed with a DEAE-Sepharose column. The anti-HIV-1 activity of each eluting fraction was tested by MTT assay. The antiviral factor was eluted in 1.0–2.0 M NaCl. (B) *Sukumo* extract was analyzed by SDS-PAGE. 0.4 mg of *Sukumo* extract was separated with 15% SDS-PAGE. The gel was stained with silver reagent for protein analysis. The anti-HIV-1 activities of extracts from SDS-gel fractions were tested by MTT assay.

Table 1
Compound properties of *Sukumo* extract

Amino acid (%)	Carbohydrate ^a	Molar ratio	Element	Percentage (%)
0.002	Arabinose	5.1	H	4.14
	Xylose	1	C	37.16
	Mannose	2.1	N	6.66
	Galactose	3.3	S	1.14
	Glucose	2.6		
	Rhamnose	Trace		

^a The *Sukumo* extract was hydrolyzed with 1 M H₂SO₄ at 100 °C for 6 h, and then the solution was applied on Supelco SP-2380 column and was analyzed with Shimadzu gas cells chromatograph GC-14B.

Sukumo extract (Table 1). The anti-viral factor in *Sukumo* extract was stable under a wide range of pH conditions. As shown in Table 2, the anti-viral activity of *Sukumo* extract was not reduced after treatment with 6N H₂SO₄, 1N HCl or NaIO₄, but the value of EC₅₀ (1.095 µg/ml) was somewhat decreased when it was treated with 1N NaOH. The activity was also not lost after being heated at 121 °C for 20 min and was not inactivated by protease (trypsin, proteinase K and pronase) digestion. Finally, we addressed whether the anti-HIV-1 activities of *Sukumo* extract, heparin and dextran sulfate were abrogated after they were treated with acid. When *Sukumo* extract was boiled at 100 °C in 6N H₂SO₄ and 1N HCl for 6 h the 50% effective concentration (EC₅₀) against HIV-1 was essentially unaffected. In sharp contrast, when

Table 2
Effect of various physico-chemical treatments on anti-HIV-1 (III_B) activity of *Sukumo* extract in MT-4

Treated with	Compound ^a (EC ₅₀ µg/ml)		
	<i>Sukumo</i> extract	Heparin	Dextran sulfate (MW 500,000)
Untreated	0.5891	8.2095	0.7016
121 °C 20 min	0.5166	ND ^f	ND ^f
Trypsin ^b	0.6686	ND	ND
Proteinase K ^b	0.5727	ND	ND
Pronase ^b	0.4736	ND	ND
NaOH ^c	1.0954	ND	ND
NaIO ₄ ^d	0.5832	ND	ND
H ₂ SO ₄ treated ^e	0.4155	>940	ND
HCl treated ^e	0.7707	ND	>1000

^a The 50% effective concentration was determined by MTT assay using HIV-1 (III_B) strain and MT-4 cells.

^b The *Sukumo* extract was digested by trypsin (Sigma) (0.5–1 mg/ml at a final concentration), proteinase K (100 ng/ml) and pronase (Fluka) (0.2 mg/ml) at 37 °C for 30 h. The digestions were terminated by boiling the solution for 20 min at 100 °C.

^c The *Sukumo* extract was boiled at 100 °C for 6 h in the presence of 1N NaOH.

^d The *Sukumo* extract was incubated at 4 °C for 40 h in the presence of 100 mM NaIO₄. After treatment, the *Sukumo* extract was precipitated with 2 volumes of ethanol and resuspended in 1 volume of H₂O.

^e Each compound was boiled at 100 °C for 6 h in the presence of 6N H₂SO₄ or for 2 h in the presence of 1N HCl. After treatment, pH was adjusted to 7.5.

^f ND: not determined.

heparin was boiled at 100 °C in 6N H₂SO₄ for 6 h or dextran sulfate in 1N HCl for 2 h, the 50% effective concentrations against HIV-1 were >940 and >1000 µg/ml by MTT assay, while those of the untreated samples were 8.2095 and 0.7707 µg/ml, respectively (Table 2).

4. Discussion

Sukumo extract potently and selectively inhibited HIV-1 replication in vitro. The compound was also evaluated for activity against various virus species with or without an envelope including vesicular stomatitis virus G protein enveloped HIV-1 pseudotyped type virus. Whereas *Sukumo* extract was active against herpes simplex virus, it was devoid of any activity against influenza A virus, SARS virus and a non-enveloped poliovirus.

Based on the current knowledge of HIV, several stages of the viral life cycle are potentially vulnerable to inhibitors. These can be divided into the entry steps and post-entry steps. In this study, we have demonstrated by several different techniques that *Sukumo* extract inhibits the HIV-1 infectious process at the cell entry step. The data presented in Fig. 3 indicate that *Sukumo* extract is able to block viral binding to target cells and inhibits virus-induced cell–cell fusion. Furthermore, a time-course experiment showed that the full protective activity of *Sukumo* extract was achieved when the compound was present during the 2-h virus adsorption period, but none of the effect was seen when the compound was incubated with the cells prior to viral infection. Also, the extract did not suppress the viral replication after the virus had entered the cells. Thus, *Sukumo* extract interferes with an early event of the virus replication cycle, most presumably the viral adsorption step.

Two classes of cell surface molecules, CD4 and chemokine receptors, as well as CCR5 or CXCR4, are often viewed as HIV coreceptors which mediate HIV-1 entry. We found that the down-modulation of HIV-1 receptor CD4 or co-receptor CCR5 in target cells was induced by the *Sukumo* extract. However, the inhibitory activity was rather weak. In addition, this activity of *Sukumo* extract was lost if the cells were washed prior to addition of antibody, indicating that the compounds can only weakly associate with the cell surface. Therefore, the results cannot perfectly explain why the *Sukumo* extract is able to block virus entry of HIV so efficiently, especially the R5 HIV-1 virus.

The effect of *Sukumo* extract on the viral binding process was assessed directly, using a chromatography method (Fig. 4). The results show that *Sukumo* extract was bound to HIV-1 and was separated along with the larger virus particle fraction from a gel filtration column. From this study we hypothesized that *Sukumo* extract exerts its anti-HIV activity by binding to the viral envelope glycoprotein. This results in prevention of virus attachment to the cell surface receptor or co-receptor, whereby interference with early adsorption and entry into the HIV replicative cycle. These findings are

consistent with the hypothesis that *Sukumo* extract interferes with virions rather than cell function. It might also explain why *Sukumo* extract is less toxic to target cells in vitro.

The biochemical features of water extract of *Sukumo* prepared from *Polygonum tinctorium* that selectively inhibited the replication of HIV-1 were studied. The anti-viral activity was extracted from *Sukumo* in a variety of ways, using water and organic solvents (hexane, chloroform, acetone and ethanol). Inhibitory activity was found in the aqueous extracts, whereas the extracts by organic solvents did not show any anti-HIV activity. Indigo, a staining ingredient and tryptanthrin, a low molecular weight component from *Polygonum tinctorium*, also did not exhibit any anti-HIV activity (data not shown).

The main fraction of anti-HIV activity was eluted from the DEAE-Sephacel column, a negative ion-exchange column at higher molar (1.0–2.0) NaCl. This result indicate that the active factor(s) is highly anionic. It was also confirmed that the anti-HIV compound(s) consist of phenolic substructure by $\text{FeCl}_3\text{-K}_3\text{Fe}(\text{CN})_6$ staining (Barton et al., 1952) (data not shown) and a polysaccharide containing sulfur atom by sugar analysis and elemental analysis, respectively (Table 1). The factor was estimated to be a high molecular weight compound of 10,000–50,000 by Sephadex G-75 gel-filtration analysis (data not shown) and an SDS-gel of *Sukumo* extract (Fig. 6B). No protein was detected in the water extract of *Sukumo* with SDS-PAGE/silver staining. The data confirm our observation that the inhibitory activity of *Sukumo* extract was not inactivated by protease digestion or heating at 121 °C for 20 min. Furthermore, boiling of the *Sukumo* extract in the presence of 1N HCl, 6N H_2SO_4 and 1N NaOH for 6 h did not result in any loss of this activity. Similarly, it was not inactivated by NaIO_4 treatment (Nakashima et al., 1987b), which breaks down carbohydrates (Table 2). This suggests that the sugar backbone is not essential for the anti-HIV activity of the *Sukumo* extract. The pharmaceutical value of the *Sukumo* extract is likely to be further enhanced by its stability over a wide range of pH values, as shown by the heating at 121 °C 20 min and treatment with acid and alkaline conditions. Since the anti-HIV-1 activity of *Sukumo* was higher than that of fresh leaves (data not shown), the possibility that the active substances were derived from bacteria could not be excluded.

We compared difference between representative sulfated polysaccharides and *Sukumo* extract for their susceptibility to acid treatment. The anti-HIV-1 effect was clearly abrogated by this treatment in the case of dextran sulfate and heparin, but not *Sukumo* extract (Table 2). The anti-HIV-1 activity of heparin was completely destroyed by 6N H_2SO_4 treatment as in the case of 1N HCl treatment of dextran sulfate. Unlike epigallocatechin gallate, a polyphenolic substance from green tea (Suzutani et al., 2003; Yamaguchi et al., 2002), *Sukumo* extract did not exert any anti-HIV-1 activity on the post-virus entry process. Further work on the characterization of the *Sukumo* extract and its potency as an anti-viral candidate drug is in progress.

Acknowledgements

The authors thank Dr. Fumio Shaku for performing the infection of HSV-1 experiments and gift of wild-type herpes simplex virus 1 and Vero cells. This work was supported by grants from the Ministry of Education, Science, and Culture and the Ministry of Health, Labor, and Welfare of Japan. The manuscript was reviewed prior to submission by Pacific Edit.

References

- Baba, M., Pauwels, R., Balzarini, J., Arnout, J., Desmyter, J., De Clercq, E., 1988. Mechanism of inhibitory effect of dextran sulfate and heparin on replication of human immunodeficiency virus in vitro. *Proc. Natl. Acad. Sci. U.S.A.* 85, 6132–6136.
- Bartolini, B., Di Caro, A., Cavallaro, R.A., Liverani, L., Mascellani, G., La Rosa, G., Marianelli, C., Muscillo, M., Benedetto, A., Cellai, L., 2003. Susceptibility to highly sulphated glycosaminoglycans of human immunodeficiency virus type 1 replication in peripheral blood lymphocytes and monocyte-derived macrophages cell cultures. *Antiviral Res.* 58, 139–147.
- Barton, G.M., Evans, R.S., Gardner, J.A.F., 1952. Paper chromatography of phenolic substances. *Nature* 170, 249–250.
- Honda, G., Tabata, M., 1979. Isolation of antifungal principle tryptanthrin, from *Strobilanthes cusia* O. Kuntze. *Planta Med.* 36, 85–86.
- Ichiyama, K., Yokoyama-Kumakura, S., Tanaka, Y., Tanaka, R., Hirose, K., Bannai, K., Edamatsu, T., Yanaka, M., Niitani, Y., Miyano-Kurosaki, N., Takaku, H., Koyanagi, Y., Yamamoto, N., 2003. A duodenally absorbable CXC chemokine receptor 4 antagonist, KRH-1636, exhibits a potent and selective anti-HIV-1 activity. *Proc. Natl. Acad. Sci. U.S.A.* 100, 4185–4190.
- Kataoka, M., Hirata, K., Kunikata, T., Ushio, S., Iwaki, K., Ohashi, K., Ikeda, M., Kurimoto, M., 2001. Antibacterial action of tryptanthrin and kaempferol, isolated from the indigo plant (*Polygonum tinctorium* Lour.), against *Helicobacter pylori*-infected Mongolian gerbils. *J. Gastroenterol.* 36, 5–9.
- Kim, H.M., Hong, D.R., Lee, E.H., 1998. Inhibition of mast cell-dependent anaphylactic reactions by the pigment of *Polygonum tinctorium* (Chung-Dae) in rats. *Gen. Pharmacol.* 31, 361–365.
- Koya-Miyata, S., Kimoto, T., Micallef, M.J., Hino, K., Taniguchi, M., Ushio, S., Iwaki, K., Ikeda, M., Kurimoto, M., 2001. Prevention of azoxymethane-induced intestinal tumors by a crude ethyl acetate-extract and tryptanthrin extracted from *Polygonum tinctorium* Lour. *Anticancer Res.* 21, 3295–3300.
- Lin, Y.L., Mettling, C., Portales, P., Reynes, J., Clot, J., Corbeau, P., 2002. Cell surface CCR5 density determines the postentry efficiency of R5 HIV-1 infection. *Proc. Natl. Acad. Sci. U.S.A.* 99, 15590–15595.
- Miyake, M., Arai, N., Ushio, S., Iwaki, K., Ikeda, M., Kurimoto, M., 2003. Promoting effect of kaempferol on the differentiation and mineralization of murine pre-osteoblastic cell line MC3T3-E1. *Biosci. Biotechnol. Biochem.* 67, 1199–1205.
- Moore, J.P., Stevenson, M., 2000. New targets for inhibitors of HIV-1 replication. *Nat. Rev. Mol. Cell Biol.* 1, 40–49.
- Moulard, M., Lortat-Jacob, H., Mondor, I., Roca, G., Wyatt, R., Sodroski, J., Zhao, L., Olson, W., Kwong, P.D., Sattentau, Q.J., 2000. Selective interactions of polyanions with basic surfaces on human immunodeficiency virus type 1 gp120. *J. Virol.* 74, 1948–1960.
- Nakashima, H., Kido, Y., Kobayashi, N., Motoki, Y., Neushul, M., Yamamoto, N., 1987a. Purification and characterization of an avian myeloblastosis and human immunodeficiency virus reverse transcriptase inhibitor, sulfated polysaccharides extracted from sea algae. *Antimicrob. Agents Chemother.* 31, 1524–1528.

- Nakashima, H., Kido, Y., Kobayashi, N., Motoki, Y., Neushul, M., Yamamoto, N., 1987b. Antiretroviral activity in a marine red alga: reverse transcriptase inhibition by an aqueous extract of *Schizymenia pacifica*. *J. Cancer Res. Clin. Oncol.* 113, 413–416.
- Nakashima, H., Yoshida, O., Baba, M., De Clercq, E., Yamamoto, N., 1989. Anti-HIV activity of dextran sulphate as determined under different experimental conditions. *Antiviral Res.* 11, 233–246.
- Nakashima, H., Murakami, T., Yamamoto, N., Sakagami, H., Tanuma, S., Hatano, T., Yoshida, T., Okuda, T., 1992. Inhibition of human immunodeficiency viral replication by tannins and related compounds. *Antiviral Res.* 18, 91–103.
- Santhosh, K.C., Paul, G.C., De Clercq, E., Pannecouque, C., Witvrouw, M., Loftus, T.L., Turpin, J.A., Buckheit Jr., R.W., Cushman, M., 2001. Correlation of anti-HIV activity with anion spacing in a series of cosalane analogues with extended polycarboxylate pharmacophores. *J. Med. Chem.* 44, 703–714.
- Suzutani, T., Ogasawara, M., Yoshida, I., Azuma, M., Knox, Y.M., 2003. Anti-herpesvirus activity of an extract of *Ribes nigrum* L. *Phytother. Res.* 17, 609–613.
- Witvrouw, M., De Clercq, E., 1997. Sulfated polysaccharides extracted from sea algae as potential antiviral drugs. *Gen. Pharmacol.* 29, 497–511.
- Yamaguchi, K., Honda, M., Ikigai, H., Hara, Y., Shimamura, T., 2002. Inhibitory effects of (–)-epigallocatechin gallate on the life cycle of human immunodeficiency virus type 1 (HIV-1). *Antiviral Res.* 53, 19–34.
- Ylisastigui, L., Bakri, Y., Amzazi, S., Gluckman, J.C., Benjouad, A., 2000. Soluble glycosaminoglycans do not potentiate RANTES antiviral activity on the infection of primary macrophages by human immunodeficiency virus type 1. *Virology* 278, 412–422.
- Zacharius, R.M., Zell, T.E., Morrison, J.H., Woodlock, J.J., 1969. Glycoprotein staining following electrophoresis on acrylamide gels. *Anal Biochem.* 30, 148–152.

Identification of Novel Low Molecular Weight CXCR4 Antagonists by Structural Tuning of Cyclic Tetrapeptide Scaffolds

Hirokazu Tamamura,^{*,‡,§} Takanobu Araki,[‡] Satoshi Ueda,[‡] Zixuan Wang,[§] Shinya Oishi,[‡] Ai Esaka,[‡] John O. Trent,^{||} Hideki Nakashima,[‡] Naoki Yamamoto,[‡] Stephen C. Peiper,[§] Akira Otaka,[‡] and Nobutaka Fujii^{*,‡}

Graduate School of Pharmaceutical Sciences, Kyoto University, Sakyo-ku, Kyoto 606-8501, Japan; Institute of Biomaterials and Bioengineering, Tokyo Medical and Dental University, Chiyoda-ku Tokyo 101-0062, Japan; Medical College of Georgia, Augusta, Georgia 30912; James Graham Brown Cancer Center, University of Louisville, Louisville, Kentucky 40202; St. Marianna University, School of Medicine, Miyamae-ku, Kawasaki 216-8511, Japan; and Tokyo Medical and Dental University, School of Medicine, Bunkyo-ku, Tokyo 113-8519, Japan

Received January 5, 2005

A highly potent CXCR4 antagonist, compound **2**, was previously found by using two orthogonal cyclic pentapeptide libraries involving conformation-based and sequence-based libraries based on the pharmacophore of a 14-mer peptidic antagonist, **1**. Herein, cyclic tetrapeptides derived from replacements of the dipeptide unit (Nal-Gly) with a γ -amino acid and pseudopeptides cyclized by disulfide and olefin bridges were synthesized to find novel scaffold structures different from that of cyclic pentapeptides. These compounds contain a reduced number of peptide bonds compared to compound **2**. Furthermore, several analogues with chemical modification of the side chain of Arg⁴ in **2** were also prepared. From these, several new leads possessing high to moderate CXCR4-antagonistic activity were characterized.

Introduction

The chemokine receptor, CXCR4, is a seven transmembrane (7TM) GPCR that transduces signals of its endogenous ligand, stromal cell-derived factor-1 (SDF-1).^{1–4} The SDF-1/CXCR4 system plays an important role in the migration of progenitors during embryologic development of the cardiovascular, hemopoietic, and central nervous systems. Recently, this system has been shown to be involved in several diseases, including HIV infection,⁵ cancer metastasis/progression,^{6–20} and rheumatoid arthritis (RA).²¹ CXCR4 was initially identified as a coreceptor that is utilized in T cell line-tropic (X4-) HIV-1 entry.⁵ Müller et al. reported that CXCR4 and another chemokine receptor, CCR7, are highly expressed in human breast cancer cells, while SDF-1 and a CCR7 ligand, CCL21, are highly expressed in lymph nodes, bone marrow, lung, and liver, which represent the primary metastatic destinations of breast cancer, suggesting that the SDF-1/CXCR4 system might determine the metastatic destination of tumor cells.⁶ Recently, this system has been recognized to be involved in the metastasis of several types of cancers, such as pancreatic cancer,^{7,8} melanoma,^{6,9} prostate cancer,¹⁰ kidney cancer,¹¹ neuroblastoma,¹² non-Hodgkin's lymphoma,¹³ lung cancer,¹⁴ ovarian cancer,^{15,16} multiple myeloma,¹⁷ chronic lymphocytic leukemia,¹⁸ acute lymphoblastic leukemia,¹⁹ and malignant brain tumor.²⁰ Nanki et al. reported that the memory T cells highly express CXCR4 and the SDF-1 concentration is extremely high in the synovium of RA patients, and that

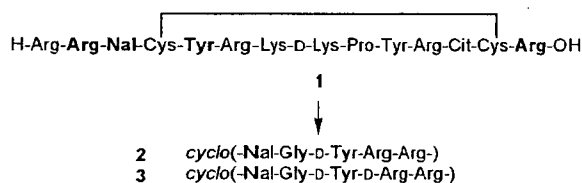


Figure 1. Reduction of the molecular size of a peptide **1** to cyclic pentapeptides **2** and **3**. Bold residues are the indispensable residues of **1** for the expression of strong CXCR4-antagonistic activity.

SDF-1 stimulates migration of the memory T cells and inhibits T cell apoptosis, indicating that the SDF–CXCR4 interaction plays a critical role in T cell accumulation in the RA synovium.²¹ Thus, CXCR4 is thought to be an important therapeutic target for these diseases. Compound **1** and its analogues, 14-mer peptides, were previously found to be specific CXCR4 antagonists that were characterized as HIV-entry inhibitors,²² anticancer-metastatic agents^{8,23} and anti-RA agents.²⁴ Arg², L-3-(2-naphthyl)alanine (Nal)³, Tyr⁵, and Arg¹⁴ were proven to constitute the critical pharmacophores of **1** (Figure 1).²⁵ The efficient utilization of two orthogonal cyclic pentapeptide libraries consisting of conformation-based and sequence-based libraries involving the critical residues of **1** led to molecular-size reduction of **1** and discovery of cyclic pentapeptides, **2** and **3**, which have strong CXCR4-antagonistic activity, comparable to that of **1**.²⁶ In this paper, we describe the fine-tuning of ring structures based on cyclic pentapeptide templates,^{27–34} and chemical modifications of side chains for an increase in potency and a reduction of the peptide characteristics of **2**.³⁵

Chemistry

γ -Amino Acid-Containing Cyclic Tetrapeptides (**11a–d**). Requisite *N*^ε-Fmoc- γ -amino acids, (2*E*,4*S*)-*N*^ε-

* Corresponding authors. Tel: +81 75 753 4551, Fax: +81 75 753 4570, e-mail: tamamura@pharm.kyoto-u.ac.jp and nfujii@pharm.kyoto-u.ac.jp.

[‡] Kyoto University.

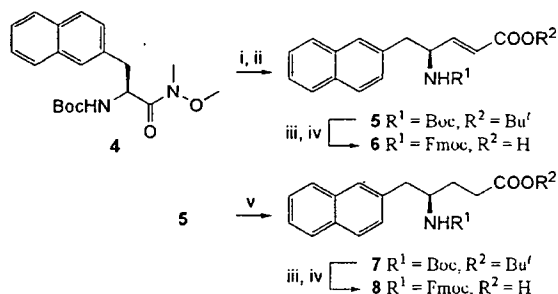
[§] Institute of Biomaterials and Bioengineering.

^{||} Medical College of Georgia.

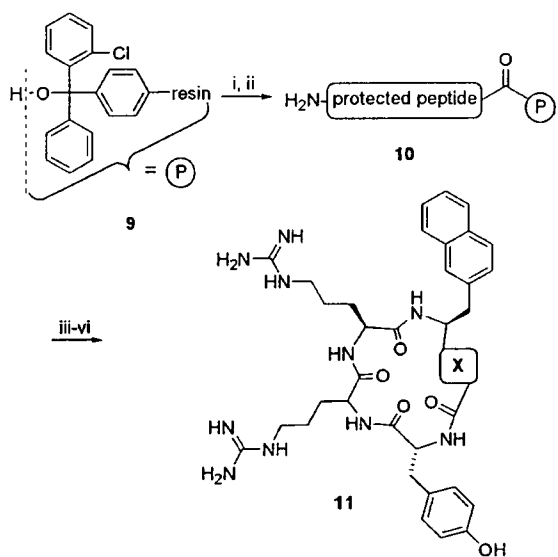
[§] University of Louisville.

[‡] St. Marianna University.

[‡] School of Medicine.

Scheme 1^a

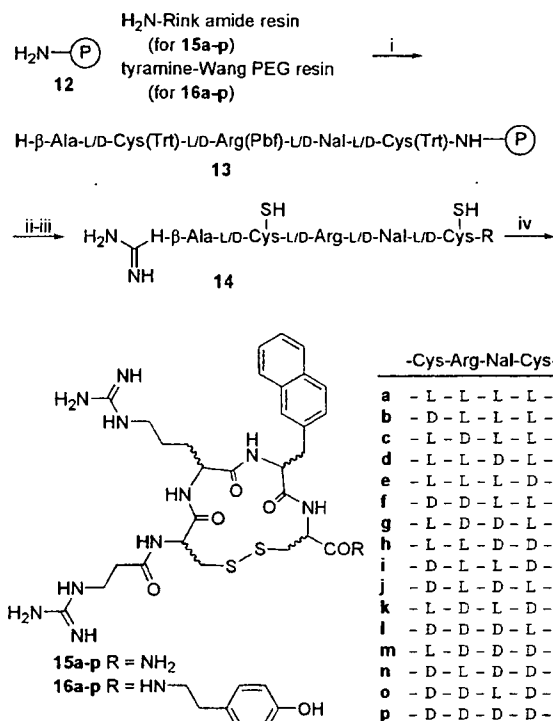
^a Reagents: (i) DIBAL-H; (ii) (EtO)₂P(O)CH₂CO₂Bu', LiCl, DIPEA; (iii) 95% aqueous TFA; (iv) Fmoc-OSu, Et₃N; (v) H₂, Pd/C.

Scheme 2^a

Compd.	Sequence (cyclic)	X
11a	(-γ-Nal ¹ -D-Tyr ² -D-Arg ³ -Arg ⁴ -)	-CH ₂ -CH ₂ -
11b	(-γ-Nal ¹ -D-Tyr ² -Arg ³ -Arg ⁴ -)	-CH ₂ -CH ₂ -
11c	(-γ-(E)-Nal ¹ -D-Tyr ² -D-Arg ³ -Arg ⁴ -)	-CH=CH-
11d	(-γ-(E)-Nal ¹ -D-Tyr ² -Arg ³ -Arg ⁴ -)	-CH=CH-

^a Reagents: (i) 6 or 8, DIPEA, DMF/CH₂Cl₂; (ii) Fmoc-based SPPS; (iii) AcOH/TFE/CH₂Cl₂; (iv) DPPA, NaHCO₃; (v) basic alumina column; (vi) 95% aqueous TFA.

Fmoc-4-amino-5-naphthalen-2-yl-pent-2-enoic acid (γ-(E)-Nal) **6** and (4R)-N^γ-Fmoc-4-amino-5-naphthalen-2-yl-pentanoic acid (γ-Nal) **8**, were synthesized according to Scheme 1. Boc-Nal-NMe(OMe) **4** was treated with DIBAL followed by modified Horner–Wadsworth–Emmons olefination to yield Boc-γ-(E)-Nal-OBu' **5**. N^α-Fmoc-protection after the cleavage of the N^γ-Boc and Bu' groups of **5** with TFA afforded a desired compound, Fmoc-γ-(E)-Nal-OH **6**. Hydrogenation of **5** obtained a reduced compound, **7**, which was similarly converted to another desired compound, Fmoc-γ-Nal-OH **8**. The protected peptide resin **10** was constructed by general Fmoc-based solid-phase synthesis on a (2-chloro)trityl resin **9**, in which the above γ-amino acid, **6** or **8**, was introduced as a C-terminal residue by DIPEA in DMF/CH₂Cl₂ (Scheme 2). Cleavage of the linear peptide from the resin with AcOH/TFE/CH₂Cl₂ (1:1:3 (v/v)) followed by cyclization with diphenylphosphoryl azide (DPPA)

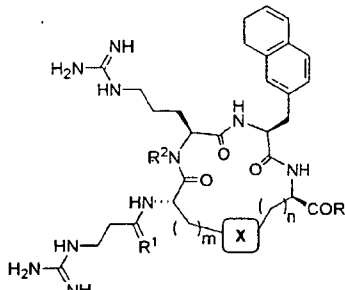
Scheme 3^a

^a Reagents: (i) Fmoc-based SPPS; (ii) 1H-pyrazole-1-carboxamide hydrochloride, DIPEA; (iii) EDT/H₂O/TFA; (iv) aqueous AcONH₄ pH 8.

and NaHCO₃, subsequent deprotection with TFA and HPLC purification gave the desired cyclic peptide **11**.²⁶

Disulfide-Bridged Cyclic Peptides (15a–p and 16a–p). The protected peptide resin was constructed by general Fmoc-based solid-phase synthesis on an NH₂-Rink amide resin (for **15a–p**) or a tyramine-Wang PEG resin (for **16a–p**) **12** (Scheme 3). Fmoc-β-Ala-OH was condensed to the N-terminus of the protected resin as the final residue. After deprotection of the Fmoc group, N-guanylation of the resulting free β-amino group with 1H-pyrazole-1-carboxamide hydrochloride and DIPEA, followed by cleavage from the resin and removal of the 2,2,4,6,7-pentamethyldihydrobenzofuran-5-sulfonyl (Pbf) and Trt groups with EDT/H₂O/TFA, gave the crude reduced peptide (2SH-peptide) **14**. Subsequent air-oxidation of the crude 2SH-peptide **14** and HPLC purification yielded the desired disulfide peptide **15** or **16**.

Disulfide-Bridged Cyclic Peptides (15q and 16q). The protected peptide resin was constructed on an Fmoc-NH-Rink amide resin (for **15q**) or an Fmoc-tyramine-Wang PEG resin (for **16q**) in the same manner as in the synthesis of **15e** or **16e** (Table 1). Reductive amination of the N-terminal amino group of the protected resin with N-Fmoc-3-aminopropanal and NaBH(OAc)₃,³⁶ followed by removal of the Fmoc group and the subsequent N-guanylation of the resulting free amino group in the same manner as in the synthesis of **15e** or **16e**, obtained the protected pseudo-peptide resin. Cleavage from the resin and removal of the Pbf and Trt groups, the subsequent air-oxidation, and HPLC purification were performed in the same manner as in the

Table 1. Inhibitory Activity of Disulfide/Olefin-Bridged Cyclic Peptides against SDF-1 Binding to CXCR4


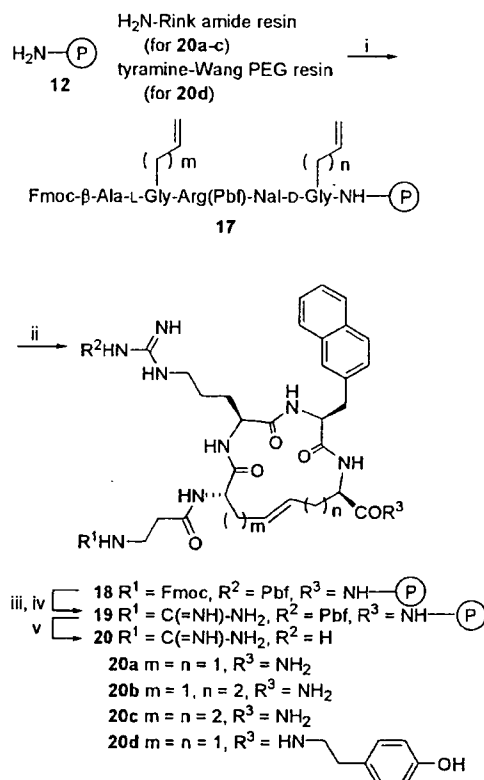
compd	m	n	X	R ¹	R ²	R ³	IC ₅₀ ± SD (μ M) ^a
15e	1	1	S-S	O	H	NH ₂	0.69 ± 0.40
16e	1	1	S-S	O	H	tyramine	0.53 ± 0.28
15q	1	1	S-S	H ₂	H	NH ₂	ca. 1
16q	1	1	S-S	H ₂	H	tyramine	ca. 1
15r	1	1	S-S	O	Me	NH ₂	>10
16r	1	1	S-S	O	Me	tyramine	>10
20a	1	1	(E)-CH=CH	O	H	NH ₂	1-10
20b	1	2	(E)-CH=CH	O	H	NH ₂	1-10
20c	2	2	(E)-CH=CH	O	H	NH ₂	1-10
20d	1	1	(E)-CH=CH	O	H	tyramine	1-10
2							0.0043 ± 0.0012
3							0.0084 ± 0.0038

^a IC₅₀ values are based on the inhibition of [¹²⁵I]-SDF-1 binding to CXCR4 transfectants of CHO cells. All data with standard deviation (SD) are the mean values for at least three independent experiments.

synthesis of **15e** or **16e** to yield the desired pseudo-peptide, **15q** or **16q**.

Disulfide-bridged Cyclic Peptides (15r and 16r). The protected peptide resin was constructed on an Fmoc-NH-Rink amide resin (for **15r**) or an Fmoc-tyramine-Wang PEG resin (for **16r**) (Table 1). *N*^α-Methylation of the Arg(Pbf) residue in the protected resin was performed by the Fukuyama-Mitsunobu reaction.³⁷ *N*^α-*o*-Nitrobenzenesulfonyl (Ns) protection of H-Arg(Pbf)-Nal-D-Cys-NH-Rink amide (or -tyramine-Wang PEG) resin and the subsequent *N*^α-methylation with MeOH, Ph₃P, and diethyl azodicarboxylate (DEAD) were followed by removal of the *N*^α-Ns group with DBU and 2-mercaptoethanol. The next residue Fmoc-D-Tyr-(Bu^t)-OH was condensed to the secondary *N*^α-amino group of the MeArg(Pbf) residue on the protected resin by using HATU, HOAt, and DIPEA. N-Guanylation, cleavage, deprotection, air-oxidation, and HPLC purification were subjected to yield the desired peptide, **15r** or **16r**.

Olefin-Bridged Cyclic Peptides (20a-d). The protected peptide resin was constructed on an NH₂-Rink amide resin (for **20a-c**) or an Fmoc-tyramine-Wang PEG resin (for **20d**) (Scheme 4) **12**. D-2-Allylglycine³⁸ (for **20a** or **20d**) or Fmoc-D-2-homoallylglycine^{39,40} (for **20b** or **20c**) was used as the C-terminal residue, while Fmoc-L-2-allylglycine⁴¹ (for **20a**, **20b**, or **20d**) or Fmoc-L-2-homoallylglycine⁴² (for **20c**) was used as the N-terminal second residue. Fmoc-β-Ala-OH was condensed to the N-terminus of the protected resin as the final residue. The protected peptide resin **17** was subjected to ring-closing olefin metathesis with Grubbs catalyst second generation⁴³ to give the cyclized peptide resin **18**. After deprotection of the Fmoc group, N-guanylation of the resulting free β-amino group, followed by treat-

Scheme 4^a

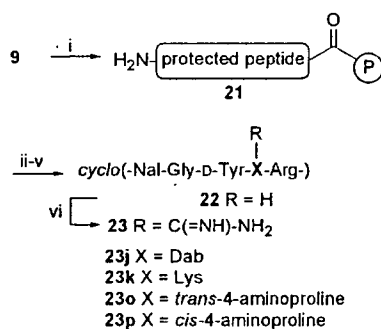
^a Reagents: (i) Fmoc-based SPPS; (ii) Grubbs catalyst 2nd generation, (iii) piperidine; (iv) 1*H*-pyrazole-1-carboxamide hydrochloride, DIPEA; (v) 1 M TMSBr-thioanisole/TFA.

ment with 1 M TMSBr-thioanisole/TFA and HPLC purification, gave the desired peptide **20**. The *E* geometry of the olefin units in **20a-d** was easily established from the coupling constants (*J* = 15.5, 15.6, 15.2, and 15.2 Hz, respectively) of the two olefinic protons by ¹H NMR analysis.

Analogues with Substitution for Arg⁴ (23a-p). Each peptide was synthesized in a general manner similar to that in the synthesis of **11a**, **23d** and **23f**: *N*^α-Methylation and coupling reaction to the *N*^α-methylated residue were performed in a manner similar to that in the synthesis of **15r**, **23j,k** and **23o,p**: After cyclization and deprotection, N-guanylation of the resulting free γ- or ε-amino group of the L-2,4-diaminobutyric acid (Dab)⁴ or Lys⁴ residue (for **23j** or **23k**, respectively) was performed with 1*H*-pyrazole-1-carboxamide hydrochloride and DIPEA (Scheme 5). N-Guanylation of the resulting free γ-amino group of the *trans*- or *cis*-4-aminoproline residue⁴⁴ (for **23o** or **23p**, respectively) was similarly performed.

Biological Results and Discussion

γ-Amino Acid-Containing Cyclic Tetrapeptides. Cyclic pentapeptides, **2** and **3**, have a Gly residue as a spacer for cyclization. To reduce the ring size, the Nal-Gly sequences of **2** and **3** were replaced by a γ-Nal or γ-(*E*)-Nal unit (Scheme 2). Among these γ-amino acid-containing cyclic tetrapeptides (**11a-d**), only **11a** [substitution of γ-Nal for Nal-Gly of **3**] showed high CXCR4-antagonistic activity (IC₅₀ = 54 nM) (Figure 2), although

Scheme 5^a

^a Reagents: (i) Fmoc-based SPPS; (ii) AcOH/TFE/CH₂Cl₂ (1:1:3 (v/v)); (iii) DPPA, NaHCO₃; (iv) basic alumina column; (v) 95% aqueous TFA; (vi) 1*H*-pyrazole-1-carboxamide hydrochloride, DIPEA.

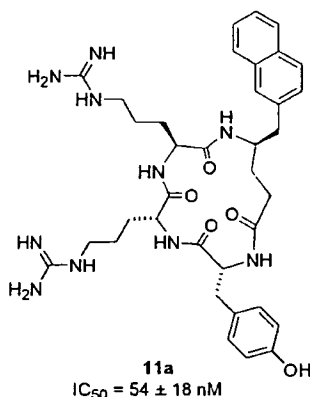


Figure 2. The structure of 11a.

this activity is 6-fold lower than that of **3**. This result suggested that the Gly residue and the amide bond of the Nal-Gly sequence are not necessary for high activity. The reason for no significant activity of **11b** [substitution of γ -Nal for Nal-Gly of **2**] (IC₅₀ > 1 μ M) cannot be well explained, however, the difference of chirality of L/D-Arg³ in **2** and **3** might cause a global conformational change of the ring. Both γ -(*E*)-Nal-substituted analogues, **11c** and **11d**, showed no significant activity (IC₅₀ > 1 μ M), suggesting that constraint of the γ -amino acid to the *E*-form might not be suitable.

Disulfide-Bridged Cyclic Peptides. To optimize the ring structures of compound **2**-derived compounds, the use of scaffold templates different from that of cyclic pentapeptides was investigated. Since the four requisite residues of **1** are disposed in close vicinity each other due to the disulfide bridge [Cys⁴-Cys¹³]⁴⁵ and cyclic peptides possessing the Arg-Arg-Nal sequence, such as **2** and **3**, showed high CXCR4-antagonistic activity, we designed and separately prepared disulfide-bridged cyclic peptide libraries consisting of the *N*-3-guanidinopropanoyl-L/D-Cys(S-)-L/D-Arg-L/D-Nal-L/D-Cys(S-)-NH₂ (or -tyramine) sequence, which included 32 compounds (2 × 2⁴ stereoisomers) (**15a-p** or **16a-p**, respectively, Scheme 3). Among these synthetic compounds, **15e** [*N*-3-guanidinopropanoyl-Cys(S-)-Arg-Nal-D-Cys(S-)-NH₂] and **16e** [*N*-3-guanidinopropanoyl-Cys(S-)-Arg-Nal-D-Cys(S-)-tyramine] exhibited moderate CXCR4-antagonistic activity (IC₅₀ = 690 and 530 nM, respectively) (Table 1), although the other compounds did not show any activity up to the concentration of 1

μ M. **15e** and **16e** have a common combination of chiralities of composed amino acids, suggesting that these compounds form similar conformations. It seems that a phenol group of **16e** is not disposed in the suitable position, since **15e** and **16e** have almost the same potencies. However, notably, L,L-chiralities of Arg-Nal are critical for high activity, as shown in **2** and **3**. The synthetic Arg side chain involving an *N*-3-guanidinopropanoyl moiety has an extra atom, compared to the original Arg side chain. This might account for the lower activity.

In addition, **15e/16e** analogues, **15q** and **16q**, in which the amide bond of *N*-3-guanidinopropanoyl-Cys was replaced by a reduced amide bond, and **15r** and **16r**, in which the α -amino group of Arg was *N*-methylated, were prepared. Substitution of the reduced amide bond for the amide bond of *N*-3-guanidinopropanoyl-Cys brought about no significant difference in potency (IC₅₀ of **15q** and **16q** = c.a. 1 μ M). This suggested that the planar character of this amide bond and the carbonyl group have little effect on potency. *N*-Methylation of Arg caused remarkable decrease in potency (IC₅₀ of **15r** and **16r** > 10 μ M), indicating that conformation surrounded by the Cys-Arg amide bond might be changed or the Cys-Arg amide proton might be required for high activity.

Olefin-Bridged Cyclic Peptides. Cyclic analogues that were bridged by an olefin instead of a disulfide in **15e** and **16e** were synthesized. C-Terminal-amidated compounds, **20a-c**, which differ in bridge length, and a C-terminal tyramide-type compound, **20d**, showed lower activity (IC₅₀ = 1–10 μ M), compared to those of **15e** and **16e** (Table 1). It is thought that the constraint of the olefin unit into the *E*-form is not an effective optimization component.

Analogues Constrained in the Peripheral Region of Arg⁴. The significant difference of activity between **23e** ([Ala⁴]-**2**, Ala-substitution for Arg⁴, IC₅₀ = 63 nM) and **23c** ([D-Ala⁴]-**2** = [D-Ala⁴]-**3**, D-Ala-substitution for L/D-Arg⁴, IC₅₀ = 230 nM) indicates a biological importance of the amide bond direction between D-Tyr and L/D-Arg. Thus, relationships between the conformation surrounded by Arg⁴ of **2** and activity were investigated. L/D-Pro-substitutions for Arg⁴ also gave the difference of activity: An L-Pro-substituted analogue, **23b**, is 4-fold stronger than a D-Pro-substituted analogue, **23a** (Table 2). *N*-Methylation of D-Ala⁴ in **23c** (IC₅₀ = 230 nM) brought about a significant increase in potency (IC₅₀ of **23d** = 42 nM), which was comparable to that of **23e** ([Ala⁴]-**2**) (IC₅₀ = 63 nM), while *N*-methylation of Ala⁴ in **23e** caused a significant decrease in potency (IC₅₀ of **23f** = 490 nM). NMR and simulated annealing molecular dynamics (SA-MD) analysis showed that the backbone structure of **23d** is very similar to that of **23e**, but different from that of **23c**, especially in the direction of the D-Tyr³-L/D-Arg amide bond (Figure 3A).⁴⁶ *N*-Methylation of D-Ala⁴ in **23c** might cause an inversion of the D-Tyr³-D-Ala⁴ amide bond (180° rotation of ϕ and ψ torsion angles) to reduce the 1,3-pseudo-allylic strain between the side chain of D-Tyr³ and the *N*-methyl group, resulting in a conformation that is similar to that of **23e**.

Ala-substitution for Arg⁴ in **2** (**23e**) did not bring about a severe decrease in potency (IC₅₀ = 63 nM),

Table 2. Inhibitory Activity of Cyclic Pentapeptides with Substitution for Arg⁴ in Compound **2** against SDF-1 Binding to CXCR4

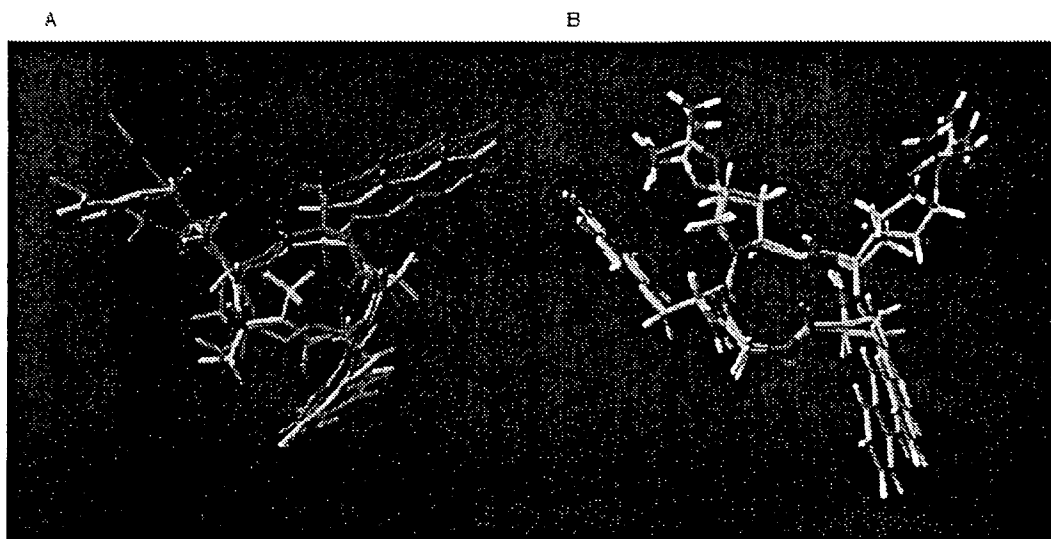
compd	sequence ^a	IC ₅₀ ± SD (μM)
23a	cyclo(-Nal-Gly-D-Tyr-D-Pro-Arg-)	1.6 ± 0.1
23b	cyclo(-Nal-Gly-D-Tyr-Pro-Arg-)	0.42 ± 0.29
23c	cyclo(-Nal-Gly-D-Tyr-D-Ala-Arg-)	0.23 ± 0.0064
23d	cyclo(-Nal-Gly-D-Tyr-D-MeAla-Arg-)	0.042 ± 0.0088
23e	cyclo(-Nal-Gly-D-Tyr-Ala-Arg-)	0.063 ± 0.013
23f	cyclo(-Nal-Gly-D-Tyr-MeAla-Arg-)	0.49 ± 0.090
23g	cyclo(-Nal-Gly-D-Tyr-Dab-Arg-)	0.016 ± 0.010
23h	cyclo(-Nal-Gly-D-Tyr-Orn-Arg-)	0.019 ± 0.011
23i	cyclo(-Nal-Gly-D-Tyr-Lys-Arg-)	0.097 ± 0.0035
23j	cyclo(-Nal-Gly-D-Tyr-g-Dab-Arg-)	0.024 ± 0.0040
23k	cyclo(-Nal-Gly-D-Tyr-g-Lys-Arg-)	0.033 ± 0.0001
23l	cyclo(-Nal-Gly-D-Tyr-Asn-Arg-)	0.27
23m	cyclo(-Nal-Gly-D-Tyr-Gln-Arg-)	0.17
23n	cyclo(-Nal-Gly-D-Tyr-Glu-Arg-)	0.61
23o	cyclo(-Nal-Gly-D-Tyr- <i>trans</i> -4-guanidino-Pro-Arg-)	0.010 ± 0.0015
23p	cyclo(-Nal-Gly-D-Tyr- <i>cis</i> -4-guanidino-Pro-Arg-)	0.0099 ± 0.0043

^a MeAla = N^α-Me-Ala.

whereas Ala-substitution for Nal¹, D-Tyr³, and Arg⁵ completely deminished activity of the parent compound (IC₅₀ > 1 μM, data not shown). These results suggest that the side chain of Arg⁴ in **2** has relatively little effect on the expression of activity, and that the spatial disposition of the δ-guanidino group of Arg⁴ might not be optimized. Thus, several analogues, in which Arg⁴ was replaced by Arg/Lys mimetics with various lengths of alkyl chains, were synthesized. Dab/L-ornithine (Orn)-substituted analogues, **23g** and **23h**, showed higher activity (IC₅₀ = 16 and 19 nM, respectively) than the Ala-substituted analogue, **23e**, whereas a Lys-substituted analogue, **23i**, was slightly weaker (IC₅₀ = 97 nM) than **23e** (Table 2). γ-N-Amidino-Dab (g-Dab)/ε-N-ami-

dino-Lys (g-Lys)-substituted analogues, **23j** and **23k**, also showed higher activity (IC₅₀ = 24 and 33 nM, respectively) than **23e**. However, these analogues were weaker than compound **2**, suggesting that Arg is the most suitable at position 4 among the Arg/Lys mimetics used in this study. Asn/Gln/Glu-substituted analogues, **23l–n**, showed a remarkable decrease in activity (IC₅₀ = 270, 170, and 610 nM, respectively). This proved that a basic functional group, such as an amino or guanidino group, is necessary for strong activity in the side chain of the amino acid at position 4, and that a hydrophilic (not basic) or acidic group is not preferable to a methyl group of Ala.

Conformationally constrained Arg mimetics, *trans*-4-guanidino-Pro and *cis*-4-guanidino-Pro (Table 2), were synthesized with the idea of fixing the backbone and side chain of Arg, according to the reported procedure.⁴⁴ These Arg mimetics were incorporated in compound **2** to determine the spatial disposition of guanidino group and increase in potency. **23o** (*trans*-4-guanidino-Pro⁴)-**2**, *trans*-4-guanidino-Pro-substitution for Arg⁴) and **23p** (*cis*-4-guanidino-Pro⁴)-**2**, *cis*-4-guanidino-Pro-substitution for Arg⁴) showed high CXCR4-antagonistic activities (IC₅₀ = 10 and 9.9 nM, respectively) that were twice as strong as that of **23j** ([g-Dab⁴]-**2**, g-Dab-substitution for Arg⁴), having the same length of the linear-type side chain of the amino acid at position 4 (IC₅₀ = 24 nM), while **23b** ([Pro⁴]-**2**, Pro-substitution for Arg⁴) did not show high activity (IC₅₀ = 420 nM). In consideration of the fact that the introduction of a pyrrolidiny ring caused a significant reduction of potency (**23a** and **23b**), it is thought that fixing the side chain effectively increased potency. From these results, we have learned that the constrained guanido group might efficiently interact with CXCR4. In addition, NMR and SA-MD analysis of **23o** and **23p** showed similar dispositions of guanidino groups of *trans/cis*-4-guanidino-Pro residues in space (Figure 3B),⁴⁶ which might be the reason for essentially no difference in potency between **23o** and **23p**.

**Figure 3.** Superimpositions of low-energy structures of **23c** (red), **23d** (green), and **23e** (blue) (A), and **23o** and **23p** (B).

Conclusion

The fine-tuning of the ring structure of compound **2** led to findings of CXCR4 antagonists involving scaffold structures that are different from cyclic pentapeptide structures: A cyclic tetrapeptide including a γ -amino acid and pseudopeptides cyclized by disulfide and olefin bridges, having a smaller number of peptide bonds compared to compound **2**, might be useful lead compounds. Furthermore, we have learned from *L/D-N^o-Me-Ala-* and *L/D-Pro-*substitutions for Arg⁴ that the direction of the carbonyl group in the *D-Tyr³-L/D-Ala⁴* amide bonds causes a remarkable effect on CXCR4-antagonistic activity. It is also clear from this study that a basic functional group, such as amino or guanidino group, in the amino acid side-chain at position **4** is indispensable for strong activity. In addition, analogues of compound **2**, where a conformationally constrained Arg mimetic, *trans-* or *cis-*4-guanidino-Pro, was incorporated at position **4**, showed high CXCR4-antagonistic activity, indicating that spatial constraint of a guanido group is important for an efficient interaction with CXCR4. These results for modifications of compound **2** provide useful insights for the future design of new low molecular weight CXCR4 antagonists, considering in connection with other CXCR4 antagonists. 47–53

Experimental Section

General. ¹H NMR spectra were recorded using a JEOL EX-270, a JEOL AL-400, or a JNM-ECA600 spectrometer at 270, 400, or 600 MHz ¹H frequency, respectively, in CDCl₃ or DMSO-*d*₆. Chemical shifts are reported in parts per million downfield from internal tetramethylsilane. Nominal (LRMS) and exact mass (HRMS) spectra were recorded on a JEOL JMS-01SG-2 or JMS-HX/HX 110A mass spectrometer. Ion-spray (IS)-mass spectrum was obtained with a Sciex APIIII triple quadrupole mass spectrometer (Toronto, Canada). Optical rotations were measured in CHCl₃ or H₂O with a JASCO DIP-360 digital polarimeter (Tokyo, Japan) or a Horiba high-sensitive polarimeter SEPA-200 (Kyoto, Japan). For flash column chromatography, silica gel 60 H (silica gel for thin-layer chromatography, Merck) and Wakogel C-200 (silica gel for column chromatography, Wako Pure Chemical Industries, Ltd., Osaka, Japan) were employed. HPLC solvents were H₂O and CH₃CN, both containing 0.1% (v/v) TFA. For analytical HPLC, a Cosmosil 5C18-AR column (4.6 × 250 mm, Nacalai Tesque Inc., Kyoto, Japan) was eluted with a linear gradient of CH₃CN at a flow rate of 1 mL/min on a Waters model 600 (Nihon Millipore, Ltd., Tokyo, Japan). Preparative HPLC was performed on a Waters Delta Prep 4000 equipped with a Cosmosil 5C18-AR column (20 × 250 mm, Nacalai Tesque Inc.) using an isocratic mode of CH₃CN at a flow rate of 15 mL/min.

[1-(*N,N*-Methoxy-methyl-carbamoyl)-2(*S*)-(2-naphthyl)-ethyl]-carbamic Acid *tert*-Butyl Ester (Boc-Nal-NMe (OMe)) (4). To a stirred solution of *L*-3-(2-naphthyl)alanine (10.0 g, 46.4 mmol) in THF–H₂O (1:1 (v/v), 200 mL) were added triethylamine (12.5 mL, 92.9 mmol) and Boc₂O (9.63 g, 44.1 mmol) at room temperature, and the mixture was stirred at this temperature overnight. The reaction mixture was concentrated under reduced pressure. The residue was extracted with EtOAc, and the extract was washed successively with saturated aqueous citric acid, aq. 5% citric acid (× 3), H₂O (× 5), and brine and dried over MgSO₄. Concentration under reduced pressure gave the crude product as a white powder, which was used directly in the following step without purification. To a solution of the crude product in DMF (150 mL) were added *N,N*-dimethylhydroxylamine hydrochloride (10.3 g, 106 mmol), triethylamine (14.3 mL, 106 mmol), HOBt (8.11 g, 52.9 mmol), and DCC (11.8 g, 53.0 mmol) at 0 °C, and the mixture was stirred at room temperature overnight. The reaction mixture was filtered, and the filtrate was concentrated

under reduced pressure. The residue was extracted with EtOAc, and the extract was washed successively with saturated aqueous citric acid, brine, saturated aqueous NaHCO₃, and brine and dried over MgSO₄. Concentration under reduced pressure followed by flash chromatography over silica gel with EtOAc–*n*-hexane (2:3) and subsequent recrystallization with Et₂O–*n*-hexane gave 12.8 g (35.7 mmol, 77% yield from *L*-3-(2-naphthyl)alanine) of **4** as colorless crystals. mp: 110–111 °C; [α]_D²⁵ +29.41 (c 0.714, CHCl₃); ¹H NMR (400 MHz, CDCl₃) δ 7.73–7.82 (m, 3H), 7.62 (s, 1H), 7.39–7.48 (m, 2H), 7.31 (dd, *J* = 8.6, 1.5 Hz, 1H), 5.17–5.24 (br d, 1H), 5.06 (br, 1H), 3.66 (s, 3H), 3.01–3.25 (m, 4H), 1.36 (s, 9H); Anal. Calcd for C₂₀H₂₅N₂O₅: C, 67.02; H, 7.31; N, 7.82. Found: C, 66.78; H, 7.47; N, 7.68.

(2*E*,4*S*)-*N*-Boc-4-amino-5-(2-naphthyl)-2-pentenoic Acid *tert*-Butyl Ester (5). To a stirred solution of **4** (7.00 g, 19.5 mmol) in CH₂Cl₂ (50 mL) was added dropwise a solution of DIBAL-H in toluene (1.0 M, 38.6 mL, 38.6 mmol) at –78 °C under argon, and the mixture was stirred at –78 °C for 2 h. The reaction was quenched with saturated aqueous citric acid (50 mL) at –78 °C, and the organic solvents were concentrated under reduced pressure. The residue was extracted with EtOAc, and the extract was washed successively with brine, aq. 50% NaHCO₃, and brine and dried over MgSO₄. Concentration under reduced pressure gave the crude aldehyde as a white solid, which was used directly in the following step without purification. To a stirred suspension of LiCl (1.65 g, 39.0 mmol) in CH₃CN (30 mL) were added (EtO)₂P(O)CH₂CO₂-Bu^t (6.31 mL, 39.0 mmol) and DIPEA (6.79 mL, 39.0 mmol) at 0 °C under argon, and the mixture was stirred at 0 °C for 1 h. The above aldehyde in CH₃CN (30 mL) was added to the mixture at 0 °C, and the mixture was allowed to warm to room temperature and stirred overnight. The reaction mixture was concentrated under reduced pressure. The residue was extracted with EtOAc, and the extract was washed successively with saturated aqueous citric acid, brine, saturated aqueous NaHCO₃, and brine and dried over MgSO₄. Concentration under reduced pressure followed by flash chromatography over silica gel with EtOAc–*n*-hexane (1:4) and subsequent recrystallization with Et₂O–*n*-hexane gave 6.05 g (15.2 mmol, 78% from **4**) of **5** as colorless crystals. mp: 135–137 °C; [α]_D²⁵ –12.84 (c 0.467, CHCl₃); ¹H NMR (400 MHz, CDCl₃) δ 7.72–7.87 (m, 3H), 7.62 (s, 1H), 7.39–7.51 (m, 2H), 7.31 (dd, *J* = 8.6, 1.7 Hz, 1H), 6.85 (dd, *J* = 15.6, 5.1 Hz, 1H), 5.81 (dd, *J* = 15.6, 1.5 Hz, 1H), 4.69 (br, 1H), 4.57 (br, 1H), 2.94–3.12 (m, 2H), 1.46 (s, 9H), 1.36 (s, 9H); Anal. Calcd for C₂₄H₃₁NO₄: C, 72.58; H, 7.86; N, 3.52. Found: C, 72.44; H, 7.86; N, 3.22.

(2*E*,4*S*)-*N*-Fmoc-4-amino-5-(2-naphthyl)-2-pentenoic Acid (6). **5** (1.00 g, 2.51 mmol) was treated with aq. 95% TFA (20 mL) at room temperature for 2.5 h. TFA was removed under reduced pressure, and the residue was dissolved in DMF–H₂O–CH₃CN (9:1:15 (v/v), 24 mL). To the stirred solution were added DIPEA (876 μL, 5.03 mmol) and Fmoc-OSu (891 mg, 2.64 mmol) at 0 °C, and the reaction mixture was stirred at room temperature for 6 h. The mixture was concentrated under reduced pressure and acidified with aq. 1 M HCl. The mixture was extracted with EtOAc, and the extract was washed successively with aq. 0.1 M HCl (× 3) and brine and dried over MgSO₄. After removal of the solvent under reduced pressure, the resulting crude product was purified by flash chromatography on silica gel with CHCl₃–MeOH (20:1) and subsequent recrystallization with (CHCl₃–*n*-hexane–MeOH) to give 345.1 mg (0.753 mmol, 30% yield from **5**) of **6** as colorless crystals. mp: 189–190 °C; [α]_D²⁵ –15.33 (c 0.326, CHCl₃); ¹H NMR (400 MHz, DMSO-*d*₆) δ 12.3 (br, 1H), 7.67–7.95 (m, 7H), 7.51–7.62 (m, 2H), 7.40–7.51 (m, 3H), 7.30–7.41 (m, 2H), 7.08–7.30 (m, 2H), 6.86 (dd, *J* = 15.6, 5.4 Hz, 1H), 5.81 (d, *J* = 15.6 Hz, 1H), 4.43–4.61 (m, 1H), 4.04–4.26 (m, 3H), 3.00–3.14 (m, 1H), 2.83–3.00 (m, 1H); LRMS (FAB), *m/z* 464 (MH⁺, base peak), 307, 179, 165, 154, 136, 141, 136, 121, 107, 91, 89, 77; HRMS (FAB), *m/z* calcd for C₃₀H₂₈NO₄ (MH⁺): 464.1862, found: 464.1853.

***N*-Boc-4(*R*)-amino-5-(2-naphthyl)-pentanoic Acid *tert*-Butyl Ester (7).** To the solution of **5** (2.50 g, 6.29 mmol) in

EtOAc (100 mL) was added 10% Pd/C (200 mg). The reaction vessel was charged with atmosphere of H₂ (balloon), and the mixture was stirred at room temperature for 8 h. Completion of the reaction was monitored by RP-HPLC. The reaction mixture was filtered through a pad of Celite, rinsing with EtOAc, and the filtrate was concentrated under reduced pressure. The resulting crude product was purified by flash chromatography on silica gel with EtOAc-*n*-hexane (1:5) and subsequent recrystallization with Et₂O-*n*-hexane to give 1.87 g (4.65 mmol, 74%) of **7** as colorless crystals. mp: 90–91 °C; $[\alpha]_D^{25}$ –20.83 (c 0.432, CHCl₃); ¹H NMR (400 MHz, CDCl₃) δ 7.71–7.86 (m, 3H), 7.62 (s, 1H), 7.38–7.52 (m, 2H), 7.34 (d, *J* = 8.1 Hz, 2H), 4.42–4.58 (br d, 1H), 2.94–3.09 (m, 1H), 2.79–2.94 (m, 1H), 2.28 (t, 2H), 1.56–1.92 (m, 2H), 1.41 (s, 9H), 1.39 (s, 9H); Anal. Calcd for C₂₄H₃₃NO₄: C, 72.15; H, 8.33; N, 3.51. Found: C, 71.92; H, 8.49; N, 3.21.

N-Fmoc-4(R)-amino-5-(2-naphthyl)-pentanoic Acid (8). **7** (1.00 g, 2.50 mmol) was treated with aq. 95% TFA (20 mL) at room temperature for 2.5 h. TFA was removed under reduced pressure, and the residue was dissolved in DMF-H₂O-THF (9:1:10 (v/v), 20 mL). To the stirred solution were added DIPEA (1.03 mL, 5.89 mmol) and Fmoc-OSu (1.29 g, 3.83 mmol) at 0 °C, and the reaction mixture was stirred at room temperature overnight. The mixture was concentrated under reduced pressure and acidified with aq. 1 M HCl. The mixture was extracted with EtOAc, and the extract was washed successively with aq. 0.1 M HCl (× 3) and brine and dried over MgSO₄. After removal of the solvent under reduced pressure, the resulting crude product was purified by flash chromatography on silica gel with CHCl₃-MeOH (20:1) and subsequent recrystallization with (CHCl₃-*n*-hexane) to give 747.6 mg (1.60 mmol, 64% yield from **7**) of **8** as colorless crystals. mp: 167–169 °C; $[\alpha]_D^{25}$ –7.31 (c 0.410, CHCl₃); ¹H NMR (400 MHz, DMSO-*d*₆) δ 7.73–7.92 (m 5H), 7.67 (s, 1H), 7.56–7.62 (m, 2H) 7.41–7.48 (m, 2H), 7.33–7.41 (m, 3H), 7.18–7.33 (m, 3H), 4.06–4.24 (m, 3H), 3.76 (br, 1H), 2.85 (d, *J* = 6.6 Hz, 2H), 2.14–2.32 (m, 2H), 1.68–1.82 (m, 1H), 1.54–1.68 (m, 1H); LRMS (FAB), *m/z* 466 (MH⁺, base peak), 179, 154, 136, 141, 136; HRMS (FAB), *m/z* calcd for C₃₀H₂₃NO₄ (MH⁺): 466.2018, found: 464.2024.

Representative Procedure for the Synthesis of γ -Amino Acid-Containing Cyclic Tetrapeptides (11a). Cl-Trt-(2-Cl) resin (1.25 mmol/g, 400 mg, 0.5 mmol) was treated with Fmoc- γ -Nal-OH (256 mg, 0.55 mmol) and DIPEA (383 μ L, 2.2 mmol) in CH₂Cl₂ (4 mL) at room temperature for 2 h to yield Fmoc- γ -Nal-Trt(2-Cl) resin (0.79 mmol/g, 97%). Protected peptide **11a** resin was manually constructed by Fmoc-based solid-phase peptide synthesis on Fmoc- γ -Nal-Trt(2-Cl) resin (0.79 mmol/g, 127 mg, 0.1 mmol). Bu^t for Tyr and Pbf for Arg were employed for side-chain protection. The protected peptide **11a** resin was treated with 1,1,1,3,3,3-hexafluoro-2-propanol (HFIP)-DCM (1:4 (v/v), 7 mL) at room temperature for 2 h. After filtration, the filtrate was concentrated under reduced pressure to give the crude protected linear peptide. To a stirred mixture of the protected peptide and *N*-methylmorpholine (54.9 μ L, 0.5 mmol) in DMF (25 mL) was added diphenylphosphoryl azide (DPPA) (53.2 μ L, 0.247 mmol) at –40 °C. The reaction mixture was stirred for 24 h with warming up to room temperature and concentrated under reduced pressure. The residue was subjected to solid-phase extraction over basic alumina in CHCl₃-MeOH (9:1) to remove inorganic salts derived from DPPA. The resulting cyclic protected peptide was treated with aq. 95% TFA (10 mL) at room temperature for 2 h. Concentration under reduced pressure and purification by HPLC gave the cyclic pseudopeptide **11a** (42.9 mg, 61% yield from Fmoc- γ -Nal-Trt(2-Cl) resin) as a freeze-dried powder.

Fmoc-tyramine-Wang PEG Resin. To a mixture of Wang PEG resin (0.33 mmol/g, 1.82 g, 0.600 mmol), Fmoc-tyramine (647 mg, 1.80 mmol), Ph₃P (472 mg, 1.80 mmol), and *N*-methylmorpholine (66.0 μ L, 0.600 mmol) in CH₂Cl₂-THF (3:1 (v/v), 16 mL) was added diisopropyl azodicarboxylate (DIAD) (40% solution in toluene, 886 μ L, 1.80 mmol) at 0 °C. The reaction mixture was stirred at room temperature for 2 d. The obtained resin was washed with THF (20 mL × 3), DMF (20

mL × 3), MeOH (20 mL × 3), CHCl₃ (20 mL × 3) and Et₂O (20 mL × 3) and dried in vacuo. The loading rate of the resin was estimated by Fmoc-quantification (0.126 mmol/g (41%).

Representative Procedure for the Synthesis of Disulfide-Bridged Cyclic Peptides (16e). Protected peptide resin was manually constructed by Fmoc-based solid-phase peptide synthesis on Fmoc-tyramine-Wang PEG resin (0.126 mmol/g, 397 mg, 0.05 mmol). Fmoc- β -Ala-OH was condensed to the N-terminal amino group of H-Cys-Arg(Pbf)-Nal-D-Cys-tyramine-Wang PEG resin, and Fmoc group was deprotected by treatment with 20% piperidine in DMF (20 min). To a mixture of the resin and DIPEA (52.5 μ L, 0.300 mmol) in DMF (5 mL) was added 1*H*-pyrazole-1-carboxamide hydrochloride (22.0 mg, 0.150 mmol) at room temperature. The reaction mixture was stirred at room temperature for 12 h. This N-guanylation procedure was repeated once again. The protected resin was treated with EDT/H₂O/TFA (2.5:2.5:95 (v/v), 6 mL) at 0 °C for 2 h. The reaction mixture was filtered, and the filtrate was concentrated by bubbling with N₂ gas. Cooled Et₂O was added to the residue, and the resulting precipitate was separated by centrifugation. The precipitate was washed with Et₂O three times. The crude peptide was dissolved in H₂O, and pH of this solution was adjusted to approximately 8 with aq. 0.28% NH₃. Air oxidation for 1 d and purification by HPLC gave the cyclic pseudopeptide **16e** (6.5 mg, 16% yield from Fmoc-tyramine-Wang PEG resin) as a freeze-dried powder.

Synthesis of 15q. Protected peptide resin was manually constructed by Fmoc-based solid-phase peptide synthesis on Fmoc-HN-Rink amide resin (0.36 mmol/g, 139 mg, 0.05 mmol). To a suspension of H-Cys-Arg(Pbf)-Nal-D-Cys-HN-Rink amide resin DCM were added *N*-Fmoc-3-aminopropanal (44.0 mg, 0.15 mmol) and NaBH(OAc)₃ (53.0 mg, 0.25 mmol) at room temperature. The mixture was stirred at room-temperature overnight. Deprotection of the Fmoc group, N-guanylation, deprotection/cleavage from the resin, air oxidation, and HPLC purification were performed by use of a procedure identical with that described for the synthesis of **16e** to yield the cyclic pseudopeptide **15q** (3.0 mg, 9% yield from Fmoc-HN-Rink amide resin) as a freeze-dried powder.

Representative Procedure for the Synthesis of Olefin-Bridged Cyclic Peptides (20a). Protected peptide resin was manually constructed by Fmoc-based solid-phase peptide synthesis on Fmoc-HN-Rink amide resin (0.29 mmol/g, 172 mg, 0.05 mmol). Fmoc- β -Ala-OH was condensed to the N-terminal amino group of H-L-2-allylGly-Arg(Pbf)-Nal-D-2-allylGly-HN-Rink amide resin. To a suspension of the protected resin in dry DCM (5 mL) was added Grubbs catalyst second generation (4.20 mg, 5.00 μ mol) at room temperature under argon. The reaction mixture was refluxed for 9 h. After removal of the organic solvent, this reaction was repeated once again for 12 h in the presence of the catalyst (21 mg, 0.025 mmol) in dry DCM (5 mL). The obtained resin was treated with 20% piperidine in DMF (20 min). To a mixture of the resin and DIPEA (52.5 μ L, 0.300 mmol) in DMF was added 1*H*-pyrazole-1-carboxamide hydrochloride (22.0 mg, 0.15 mmol) at room temperature. The reaction mixture was stirred at room temperature for 12 h. This N-guanylation procedure was repeated once again. The protected resin was treated with thioanisole (940 μ L), TFA (7.2 mL), and TMSBr (1.32 mL) at 0 °C for 2 h. The reaction mixture was filtered, and the filtrate was concentrated by bubbling with N₂ gas. Cooled Et₂O was added to the residue, and the resulting precipitate was separated by centrifugation. The precipitate was washed with Et₂O. The crude peptide was purified by HPLC to give the cyclic pseudopeptide **20a** (3.3 mg, 10% yield from Fmoc-HN-Rink amide resin) as a freeze-dried powder.

Representative Procedure for the Synthesis of Cyclic Pentapeptides (cyclo-(D-Tyr-Pro-Arg-Nal-Gly-) (23b)). Protected peptide resin was manually constructed by Fmoc-based solid-phase peptide synthesis on Fmoc-Gly-Trt(2-Cl) resin (0.741 mmol/g, 101 mg, 0.075 mmol). Bu^t for Tyr and Pbf for Arg were employed for side-chain protection. Cleavage from the resin, cyclization, deprotection, and HPLC purification were performed by use of a procedure identical with that

described for the synthesis of **11a** to yield the cyclic peptide **23b** (25.2 mg, 50% yield from Fmoc-Gly-Trt(2-Cl) resin) as a freeze-dried powder.

Representative Procedure for the Synthesis of *N*-Methylated Cyclic Pentapeptides (cyclo(*D*-Tyr-*D*-MeAla-Arg-Nal-Gly-)) (23d). According to a procedure identical with that described for the preparation of **23b**, **23d** was synthesized except for *N*-methylation of the *D*-Ala residue. *N*-Methylation was performed by the Fukuyama–Mitsunobu reaction.²⁸ To a mixture of *H*-*D*-Ala-Arg(Pbf)-Nal-Gly-Trt(2-Cl) resin (0.075 mmol) and *o*-nitrobenzenesulfonyl chloride (49.9 mg, 0.225 mmol) in CH₂Cl₂ (5 mL) was added 2,4,6-collidine (49.6 μL, 0.375 mmol) at room temperature. The reaction mixture was stirred at room temperature for 2 h, and the resin was washed successively with CH₂Cl₂ (10 mL × 3) and DMF (10 mL × 3). To a mixture of the resin, Pb₃P (98.4 mg, 0.375 mmol), and MeOH (15.2 μL, 0.375 mmol) in dry THF (5 mL) was added diethyl azodicarboxylate (DEAD) (40% solution in toluene, 170 μL, 0.375 mmol) at 0 °C. The reaction mixture was stirred at room temperature for 2 h. The resin was washed successively with THF (10 mL × 3) and DMF (10 mL × 3). To a mixture of the resin and DBU (56.1 μL, 0.375 mmol) in DMF (5 mL) was added 2-mercaptoethanol (51.4 μL, 0.750 mmol) at room temperature, and the reaction mixture was stirred at room temperature for 2 h. Subsequent condensation of the next residue (*D*-Tyr) to the secondary amino group on the resin was performed by treatment with Fmoc-*D*-Tyr(Bu^t)-OH (5 equiv), HATU (4.9 equiv), HOAt (5 equiv), and DIPEA (10 equiv) in DMF (5 mL) for 1 h (× 2). **23d** (freeze-dried powder): 3.0 mg, 6.0% yield from Fmoc-Gly-Trt(2-Cl) resin.

(2*S*,4*S*)-*N*^α-Cbz-4-*N*-Boc-aminoproline Benzyl Ester. (2*S*,4*S*)-*N*^α-Cbz-4-aminoproline benzyl ester (1.44 g, 3.93 mmol), which was prepared from (2*S*,4*S*)-*N*^α-Cbz-4-azidoproline benzyl ester according to Tamaki's procedure,³⁵ was dissolved in THF (20 mL), and Boc₂O (1.38 g, 6.31 mmol) and triethylamine (1.10 mL, 7.89 mmol) were added to the solution at 0 °C. The reaction mixture was stirred at room temperature for 7.5 h. The mixture was concentrated under reduced pressure, and the residue was extracted with Et₂O. The extract was washed successively with saturated aqueous citric acid (× 2), H₂O (× 2), and brine and dried over MgSO₄. After removal of the solvent under reduced pressure, the resulting crude product was purified by flash chromatography on silica gel with EtOAc-*n*-hexane (1:4) to give 1.70 g (3.77 mmol, 96% yield) of the title compound as a colorless oil. [α]_D²⁰ -39.47 (c 0.304, CHCl₃); ¹H NMR (400 MHz, CDCl₃) δ 7.18–7.45 (m, 10H), 4.95–5.40 (m, 5H), 4.28–4.50 (m, 2H), 3.68–3.82 (m, 1H), 3.44–3.60 (m, 1H), 2.39–2.57 (m, 1H), 1.89–2.05 (m, 1H), 1.45 (s, 9H); LRMS (FAB), *m/z* 477 (MNa⁺, base peak), 455 (MH⁺), 445, 399, 355, 91; HRMS (FAB), *m/z* calcd for C₂₅H₃₁N₂O₆ (MH⁺): 455.2182, found: 455.2186.

(2*S*,4*S*)-*N*^α-Fmoc-4-*N*-Boc-aminoproline. (2*S*,4*S*)-*N*^α-Cbz-4-*N*-Boc-aminoproline benzyl ester (1.70 g, 3.77 mmol) was dissolved in EtOH (80 mL), and 5% Pd/C (170 mg) was added to the solution. The reaction vessel was charged with atmosphere of H₂ (balloon), and the mixture was stirred at room temperature for 12 h. After removal of Pd/C by filtration, the filtrate was concentrated under reduced pressure to give the crude product as a colorless oil, which was used directly in the following step without purification. To the crude product in H₂O-THF (4:3 (v/v), 70 mL) were added triethylamine (1.41 mL, 7.55 mmol) and Fmoc-OSu (2.54 g, 7.55 mmol) in CH₃CN (10 mL) at 0 °C, and the reaction mixture was stirred at room temperature for 2 h. The mixture was acidified with saturated aqueous citric acid and concentrated under reduced pressure. The residue was extracted with EtOAc, and the extract was washed successively with saturated aqueous citric acid, H₂O (× 3), and brine and dried over MgSO₄. After removal of the solvent under reduced pressure, the resulting crude product was purified by flash chromatography on silica gel with CHCl₃-MeOH (20:1) to give 1.18 g (2.60 mmol, 69% yield) of the title compound as colorless crystals. mp: 87–89 °C; [α]_D²⁴ -33.81 (c 0.621, CHCl₃); ¹H NMR (400 MHz, DMSO-*d*₆) δ 8.30 (s, 1H), 7.82–7.97 (m, 2H), 7.57–7.75 (m, 2H), 7.25–7.49 (m,

4H), 3.93–4.36 (m, 5H), 3.60–3.75 (m, 1H), 3.05–3.21 (m, 1H), 2.32–2.58 (m, 1H), 1.67–1.90 (m, 1H), 1.44 (s, 9H); LRMS (FAB), *m/z* 451 [(M - H)⁻], 229, 155, 153, 152 (base peak); HRMS (FAB), *m/z* calcd for C₂₅H₂₇N₂O₆ [(M - H)⁻]: 451.1868, found: 451.1883.

(2*S*,4*R*)-*N*^α-Cbz-4-*N*-Boc-aminoproline Benzyl Ester. By use of a procedure identical with that described for the preparation of (2*S*,4*S*)-*N*^α-Cbz-4-*N*-Boc-aminoproline benzyl ester, (2*S*,4*R*)-*N*^α-Cbz-4-aminoproline benzyl ester (5.56 g, 15.7 mmol) was converted into 6.24 g (13.8 mmol, 88% yield) of the title compound as colorless crystals. mp: 97–99 °C; [α]_D²⁵ -47.61 (c 0.714, CHCl₃); ¹H NMR (400 MHz, CDCl₃) δ 7.15–7.43 (m, 10H), 4.93–5.27 (m, 4H), 4.56–4.70 (br, 1H), 4.37–4.54 (m, 1H), 4.21–4.35 (br, 1H), 3.78–3.89 (m, 1H), 3.30–3.50 (m, 1H), 2.12–2.34 (m, 2H), 1.45 (s, 9H); LRMS (FAB), *m/z* 477 (MNa⁺, base peak), 455 (MH⁺), 445, 399, 355, 263, 91; HRMS (FAB), *m/z* calcd for C₂₅H₃₁N₂O₆ (MH⁺): 455.2182, found: 455.2176.

(2*S*,4*R*)-*N*^α-Fmoc-4-*N*-Boc-aminoproline. By use of a procedure identical with that described for the preparation of (2*S*,4*S*)-*N*^α-Fmoc-4-*N*-Boc-aminoproline, (2*S*,4*R*)-*N*^α-Cbz-4-*N*-Boc-aminoproline benzyl ester (2.75 g, 6.10 mmol) was converted into 2.05 g (4.51 mmol, 74% yield) of the title compound as colorless crystals. mp: 85–87 °C; [α]_D²⁴ -36.92 (c 0.325, CHCl₃); ¹H NMR (400 MHz, CDCl₃) δ 8.33 (s, 1H), 7.82–7.97 (m, 2H), 7.56–7.72 (m, 2H), 7.26–7.49 (m, 4H), 3.96–4.36 (m, 4H), 3.50–3.67 (m, 1H), 3.18–3.40 (m, 2H), 1.99–2.26 (m, 2H), 1.44 (s, 9H); LRMS (FAB), *m/z* 451 [(M - H)⁻], 229, 155, 153, 151 (base peak); HRMS (FAB), *m/z* calcd for C₂₅H₂₇N₂O₆ [(M - H)⁻]: 451.1868, found: 451.1887.

Representative Procedure for the Synthesis of Cyclic Pentapeptides Containing Arginine Mimetic (cyclo(*D*-Tyr-*trans*-4-guanidino-Pro-Arg-Nal-Gly-)) (23o). According to a procedure identical with that described for the preparation of **23b**, the cyclic protected peptide was synthesized. The obtained protected peptide (0.05 mmol) was treated with aq. 95% TFA (5 mL) for 2 h at room temperature, and concentration under reduced pressure gave the crude cyclic peptide. To a mixture of the crude product and 1*H*-pyrazole-1-carboxamidino hydrochloride (22.0 mg, 0.15 mmol) in DMF (4 mL) was added DIPEA (52.3 μL, 0.300 mmol) at room temperature. The reaction mixture was stirred at room temperature for 12 h. This procedure (*N*-guanlylation of the γ -amino group of the *trans*-4-amino-Pro residue) was repeated once again. Concentration under reduced pressure and purification by HPLC gave the cyclic peptide **23o** (5.1 mg, 14% yield from Fmoc-Gly-Trt(2-Cl) resin) as a freeze-dried powder.

[¹²⁵I]-SDF-1 Binding and Displacement. Stable CHO cell transfectants expressing CXCR4 variants were prepared as described previously.³⁴ CHO transfectants were harvested by treatment with trypsin-EDTA, allowed to recover in complete growth medium (MEM- α , 100 μg/mL penicillin, 100 μg/mL streptomycin, 0.25 μg/mL amphotericin B, 10% (v/v) for four to 5 h and then washed in cold binding buffer (PBS containing 2 mg/mL BSA). For ligand binding, the cells were resuspended in binding buffer at 1 × 10⁷ cells/mL, and 100 μL aliquots were incubated with 0.1 nM of [¹²⁵I]-SDF-1 (PerkinElmer Life Sciences) for 2 h on ice under constant agitation. Free and bound radioactivity were separated by centrifugation of the cells through an oil cushion and bound radioactivity was measured with a gamma-counter (Cobra, Packard, Downers Grove, IL). Inhibitory activity of test compounds was determined based on the inhibition of [¹²⁵I]-SDF-1-binding to CXCR4 transfectants (IC₅₀).

NMR Spectroscopy (23c–e, 23o, and 23p). The peptide sample was dissolved in DMSO-*d*₆ at a concentration of 5 mM. ¹H NMR spectra of the peptides were recorded at 300 K. The assignments of the proton resonances were achieved by use of ¹H–¹H COSY spectra. ³J(H^α,H^β) coupling constants were measured from one-dimensional spectra. The mixing time for the NOESY experiments was set at 400 ms. NOESY spectra were composed of 512 real points in the F2 dimension and 256 real points, which were zero-filled to 256 points in the F1 dimension, with 144 scans per t1 increment. The cross-peak

intensities were evaluated by relative build-up rates of the cross-peaks. Temperature dependence of the chemical shifts of all of the amide protons was investigated in **23c–e**, **23o**, and **23p**. In **23c**, the temperature coefficients for all of the NH protons were large. In **23d**, the only temperature coefficient for the NH of D-Tyr³ was small, but NOE was not observed between the NaI¹ C^αH and D-Tyr³ NH. In **23e**, **23o**, and **23p**, the temperature coefficients for the NH of D-Tyr³ and Arg⁵ were small, but NOE was not observed between the NaI¹ C^αH and D-Tyr³ NH or between the D-Tyr³ C^αH and Arg⁵ NH. Thus, no hydrogen bond restraints were used in the simulated annealing calculations of **23c–e**, **23o**, and **23p**.

Calculation of Structures. The structure calculations were performed on a Silicon Graphics Origin 2000 workstation with the NMR-refine program within the Insight II/Discover package using the consistent valence force field (CVFF).⁵⁵ Pseudoatoms were defined for the methylene protons of NaI¹, D-Tyr³, Arg⁴, and Arg⁵ prochiralities of which were not identified by ¹H NMR data. The restraints, in which the Gly² α-methylene participated, were defined for the separate protons without definition of the prochiralities. The dihedral φ angle constraints were calculated based on the Karplus equation: $^3J(\text{H}^{\text{N}}, \text{H}^{\alpha}) = 6.7 \cos^2(\theta - 60) - 1.3 \cos(\theta - 60) + 1.5$.⁵⁶ Lower and upper angle errors were set to 15°. The NOESY spectrum with a mixing time of 400 ms was used for the estimation of the distance restraints between protons. The NOE intensities were classified into three categories (strong, medium, and weak) based on the number of contour lines in the cross-peaks to define the upper-limit distance restraints (2.7, 3.5, and 5.0 Å, respectively). The upper-limit restraints were increased by 1.0 Å for the involved pseudoatoms. Lower bounds between nonbonded atoms were set to their van der Waals radii (1.8 Å). These distance and dihedral angle restraints were included with force constants of 25–100 kcal/mol·Å² and 25–100 kcal/mol·rad², respectively. The 50 initial structures generated by the NMR refine program randomly were subjected to the simulated annealing calculations. The final minimization stage was achieved until the maximum derivative became less than 0.01 kcal/mol·Å² by the steepest descents and conjugate gradients methods.

Acknowledgment. This work was supported in part by a 21st Century COE Program "Knowledge Information Infrastructure for Genome Science", a Grant-in-Aid for Scientific Research from the Ministry of Education, Culture, Sports, Science and Technology, Japan, and the Japan Health Science Foundation. Computation time was provided by the Supercomputer Laboratory, Institute for Chemical Research, Kyoto University. S.U. is grateful for a Research Fellowship from the Japan Society for the Promotion of Science for Young Scientists.

Supporting Information Available: Characterization data of representative synthetic compounds and HPLC charts of **11a**, **11c**, **15e**, **16e**, **15q**, **16q**, **20a**, **20d**, **23d**, **23j**, **23o**, and **23p**. This material is available free of charge via the Internet at <http://pubs.acs.org>.

References

- Nagasawa, T.; Kikutani, H.; Kishimoto, T. Molecular cloning and structure of a pre-B-cell growth-stimulating factor. *Proc. Natl. Acad. Sci. U.S.A.* **1994**, *91*, 2305–2309.
- Bleul, C. C.; Farzan, M.; Choe, H.; Parolin, C.; Clark-Lewis, I.; Sodroski, J.; Springer, T. A. The lymphocyte chemoattractant SDF-1 is a ligand for LESTR/fusin and blocks HIV-1 entry. *Nature* **1996**, *382*, 829–833.
- Oberlin, E.; Amara, A.; Bachelier, F.; Bessia, C.; Virelizier, J.-L.; Arenzana-Seisdedos, F.; Schwartz, O.; Heard, J.-M.; Clark-Lewis, I.; Legler, D. F.; Loetscher, M.; Baggiolini, M.; Moser, B. The CXC chemokine SDF-1 is the ligand for LESTR/fusin and prevents infection by T-cell-line-adapted HIV-1. *Nature* **1996**, *382*, 833–835.
- Tashiro, K.; Tada, H.; Heilker, R.; Shirozu, M.; Nakano, T.; Honjo, T. Signal sequence trap: a cloning strategy for secreted proteins and type I membrane proteins. *Science* **1993**, *261*, 600–603.
- Feng, Y.; Broder, C. C.; Kennedy, P. E.; Berger, E. A. HIV-1 entry co-factor: Functional cDNA cloning of a seven-transmembrane, G protein-coupled receptor. *Science* **1996**, *272*, 872–877.
- Müller, A.; Homey, B.; Soto, H.; Ge, N.; Catron, D.; Buchanan, M. E.; McClanahan, T.; Murphy, E.; Yuan, W.; Wagner, S. N.; Barrera, J. L.; Mohar, A.; Verastegui, E.; Zlotnik, A. Involvement of chemokine receptors in breast cancer metastasis. *Nature* **2001**, *410*, 50–56.
- Koshiba, T.; Hosotani, R.; Miyamoto, Y.; Ida, J.; Tsuji, S.; Nakamura, S.; Kawaguchi, M.; Kobayashi, H.; Doi, R.; Hori, T.; Fujii, N.; Imamura, M. Expression of stromal cell-derived factor 1 and CXCR4 ligand receptor system in pancreatic cancer: a possible role for tumor progression. *Clin. Cancer Res.* **2000**, *6*, 3530–3535.
- Mori, T.; Doi, R.; Koizumi, K.; Toyoda, E.; Tulachan, S. S.; Ito, D.; Kami, K.; Masui, T.; Fujimoto, K.; Tamamura, H.; Hiramatsu, K.; Fujii, N.; Imamura, M. CXCR4 antagonist inhibits stromal cell-derived factor 1-induced migration and invasion of human pancreatic cancer. *Mol. Cancer Ther.* **2004**, *3*, 29–37.
- Robledo, M. M.; Bartolome, R. A.; Longo, N.; Miguel Rodriguez-Frade, J.; Mellado, M.; Longo, I.; van Muijen, G. N. P.; Sanchez-Mateos, P.; Teixido, J. Expression of functional chemokine receptors CXCR3 and CXCR4 on human melanoma cells. *J. Biol. Chem.* **2001**, *276*, 45098–45105.
- Taichman, R. S.; Cooper, C.; Keller, E. T.; Pienta, K. J.; Taichman, N. S.; McCauley, L. K. Use of the stromal cell-derived factor-1/CXCR4 pathway in prostate cancer metastasis to bone. *Cancer Res.* **2002**, *62*, 1832–1837.
- Schrader, A. J.; Lechner, O.; Templin, M.; Dittmar, K. E. J.; Machtens, S.; Mengel, M.; Probst-Kepper, M.; Franzke, A.; Wollensak, T.; Gatzlaf, P.; Atzpodien, J.; Buer, J.; Lauber, J. CXCR4/CXCL12 expression and signaling in kidney cancer. *Br. J. Cancer* **2002**, *86*, 1250–1256.
- Geminder, H.; Sagi-Assif, O.; Goldberg, L.; Meshel, T.; Rechavi, G.; Witz, I. P.; Ben-Baruch, A. A possible role for CXCR4 and its ligand, the CXC chemokine stromal cell-derived factor-1, in the development of bone marrow metastases in neuroblastoma. *J. Immunol.* **2001**, *167*, 4747–4757.
- Bertolini, F.; Dell'Agnola, C.; Mancuso, P.; Rabascio, C.; Burlini, A.; Monestiroli, S.; Gobbi, A.; Pruneri, G.; Martinelli, G. CXCR4 neutralization, a novel therapeutic approach for non-Hodgkin's lymphoma. *Cancer Res.* **2002**, *62*, 3106–3112.
- Kijima, T.; Maulik, G.; Ma, P. C.; Tibaldi, E. V.; Turner, R. E.; Rollins, B.; Sattler, M.; Johnson, B. E.; Salgia, R. Regulation of cellular proliferation, cytoskeletal function, and signal transduction through CXCR4 and c-Kit in small cell lung cancer cells. *Cancer Res.* **2002**, *62*, 6304–6311.
- Scotton, C. J.; Wilson, J. L.; Milliken, D.; Stamp, G.; Balkwill, F. R. Epithelial cancer cell migration: a role for chemokine receptors? *Cancer Res.* **2001**, *61*, 4961–4965.
- Scotton, C. J.; Wilson, J. L.; Scott, K.; Stamp, G.; Wilbanks, G. D.; Fricker, S.; Bridger, G.; Balkwill, F. R. Multiple actions of the chemokine CXCL12 on epithelial tumor cells in human ovarian cancer. *Cancer Res.* **2002**, *62*, 5930–5938.
- Sanz-Rodriguez, F.; Hidalgo, A.; Teixido, J. Chemokine stromal cell-derived factor-1α modulates VLA-4 integrin-mediated multiple myeloma cell adhesion to CS-1/fibronectin and VCAM-1. *Blood* **2001**, *97*, 346–351.
- Tsukada, N.; Burger, J. A.; Zvaifler, N. J.; Kipps, T. J. Distinctive features of "nurselike" cells that differentiate in the context of chronic lymphocytic leukemia. *Blood* **2002**, *99*, 1030–1037.
- Juarez, J.; Bradstock, K. F.; Gottlieb, D. J.; Bendall, L. J. Effects of inhibitors of the chemokine receptor CXCR4 on acute lymphoblastic leukemia cells in vitro. *Leukemia* **2003**, *17*, 1294–1300.
- Rubin, J. B.; Kung, A. L.; Klein, R. S.; Chan, J. A.; Sun, Y.-P.; Schmidt, K.; Kieran, M. W.; Luster, A. D.; Segal, R. A. A small-molecule antagonist of CXCR4 inhibits intracranial growth of primary brain tumors. *Proc. Natl. Acad. Sci. U.S.A.* **2003**, *100*, 13513–13518.
- Nanki, T.; Hayashida, K.; El-Gabalawy, H. S.; Suson, S.; Shi, K.; Girschick, H. J.; Yavuz, S.; Lipsky, P. E. Stromal cell-derived factor-1-CXC chemokine receptor 4 interactions play a central role in CD4⁺ T cell accumulation in rheumatoid arthritis synovium. *J. Immunol.* **2000**, *165*, 6590–6598.
- Tamamura, H.; Xu, Y.; Hattori, T.; Zhang, X.; Arakaki, R.; Kanbara, K.; Omagari, A.; Otaka, A.; Ibuka, T.; Yamamoto, N.; Nakashima, H.; Fujii, N. A low molecular weight inhibitor against the chemokine receptor CXCR4: a strong anti-HIV peptide T140. *Biochem. Biophys. Res. Commun.* **1998**, *253*, 877–882.
- Tamamura, H.; Hori, A.; Kanzaki, N.; Hiramatsu, K.; Mizumoto, M.; Nakashima, H.; Yamamoto, N.; Otaka, A.; Fujii, N. T140 analogs as CXCR4 antagonists identified as anti-metastatic agents in the treatment of breast cancer. *FEBS Lett.* **2003**, *550*, 79–83.

- (24) Tamamura, H.; Fujisawa, M.; Hiramatsu, K.; Mizumoto, M.; Nakashima, H.; Yamamoto, N.; Otaka, A.; Fujii, N. Identification of a CXCR4 antagonist, a T140 analog, as an anti-rheumatoid arthritis agent. *FEBS Lett.* **2004**, *569*, 99–104.
- (25) Tamamura, H.; Omagari, A.; Oishi, S.; Kanamoto, T.; Yamamoto, N.; Peiper, S. C.; Nakashima, H.; Otaka, A.; Fujii, N. Pharmacophore identification of a specific CXCR4 inhibitor, T140, leads to development of effective anti-HIV agents with very high selectivity indexes. *Bioorg. Med. Chem. Lett.* **2000**, *10*, 2633–2637.
- (26) Fujii, N.; Oishi, S.; Hiramatsu, K.; Araki, T.; Ueda, S.; Tamamura, H.; Otaka, A.; Kusano, S.; Terakubo, S.; Nakashima, H.; Broach, J. A.; Trent, J. O.; Wang, Z.; Peiper, S. C. Molecular-size reduction of a potent CXCR4-chemokine antagonist using orthogonal combination of conformation- and sequence-based libraries. *Angew. Chem., Int. Ed.* **2003**, *42*, 3251–3253.
- (27) Fukami, T.; Nagase, T.; Fujita, K.; Hayama, T.; Niiyama, K.; Mase, T.; Nakajima, S.; Fukuroda, T.; Saeki, T.; Nishikibe, M.; Ihara, M.; Yano, M.; Ishikawa, K. Structure–activity relationships of cyclic pentapeptide endothelin A receptor antagonists. *J. Med. Chem.* **1995**, *38*, 4309–4324.
- (28) Haubner, R.; Gratiyas, R.; Diefenbach, B.; Goodman, S. L.; Jonczyk, A.; Kessler, H. Structural and functional aspects of RGD-containing cyclic pentapeptides as highly potent and selective integrin $\alpha V\beta 3$ antagonists. *J. Am. Chem. Soc.* **1996**, *118*, 7461–7472.
- (29) Spatola, A. F.; Crozet, Y.; deWit, D.; Yanagisawa, M. Rediscovering an endothelin antagonist (BQ-123): A self-deconvoluting cyclic pentapeptide library. *J. Med. Chem.* **1996**, *39*, 3842–3846.
- (30) Wermuth, J.; Goodman, S. L.; Jonczyk, A.; Kessler, H. Stereoisomerism and biological activity of the selective and superactive $\alpha V\beta 3$ integrin inhibitor cyclo(-RGDfV-) and its retro-inverse peptide. *J. Am. Chem. Soc.* **1997**, *119*, 1328–1335.
- (31) Haubner, R.; Finsinger, D.; Kessler, H. Stereoisomeric peptide libraries and peptidomimetics for designing selective inhibitors of the $\alpha V\beta 3$ integrin for a new cancer therapy. *Angew. Chem., Int. Ed. Engl.* **1997**, *36*, 1374–1389.
- (32) Porcelli, M.; Casu, M.; Lai, A.; Saba, G.; Pinori, M.; Cappelletti, S.; Mascagni, P. Cyclic pentapeptides of chiral sequence DLDDL as scaffold for antagonism of G-protein coupled receptors: Synthesis, activity and conformational analysis by NMR and molecular dynamics of ITF 1565 a substance P inhibitor. *Biopolymers* **1999**, *50*, 211–219.
- (33) Oishi, S.; Kamano, T.; Niida, A.; Odagaki, Y.; Hamanaka, N.; Yamamoto, M.; Ajito, K.; Tamamura, H.; Otaka, A.; Fujii, N. Diastereoselective synthesis of new $\psi[(E)\text{-CH}=\text{CMe}]$ - and $\psi-[(Z)\text{-CH}=\text{CMe}]$ -type alkene dipeptide isosteres by organocopper reagents and application to conformationally restricted cyclic RGD peptidomimetics. *J. Org. Chem.* **2002**, *67*, 6162–6173.
- (34) Nikiforovich, G. V.; Kover, K. E.; Zhang, W.-J.; Marshall, G. R. Cyclopentapeptides as flexible conformational templates. *J. Am. Chem. Soc.* **2000**, *122*, 3262–3273.
- (35) Tamamura, H.; Hiramatsu, K.; Ueda, S.; Wang, Z.; Kusano, S.; Terakubo, S.; Trent, J. O.; Peiper, S. C.; Yamamoto, N.; Nakashima, H.; Otaka, A.; Fujii, N. Stereoselective synthesis of [L-Arg-1/D-3-(2-naphthyl)alanine]-type (E)-alkene dipeptide isosteres and its application to the synthesis and biological evaluation of pseudopeptide analogues of the CXCR4 antagonist FC131. *J. Med. Chem.* **2005**, *48*, 380–391.
- (36) Abdel-Magid, A. F.; Maryanoff, C. A.; Carson, K. G. Reductive amination of aldehydes and ketones by using sodium triacetoxyborohydride. *Tetrahedron Lett.* **1990**, *31*, 5595–5598.
- (37) Fukuyama, T.; Jow, C.-K.; Cheung, M. 2- and 4-Nitrobenzenesulfonamides: exceptionally versatile means for preparation of secondary amines and protection of amines. *Tetrahedron Lett.* **1995**, *36*, 6373–6374.
- (38) Myers, A. G.; Gleason, J. L.; Yoon, T.; Kung, D. W. Highly practical methodology for the synthesis of D- and L-R-amino acids, N-protected R-amino acids, and N-methyl-R-amino acids. *J. Am. Chem. Soc.* **1997**, *119*, 656–673.
- (39) Travins, J. M.; Etkorn, F. A. Facile synthesis of D-amino acids from an L-serine-derived aziridine. *Tetrahedron Lett.* **1998**, *39*, 9389–9392.
- (40) Biagini, S. C. G.; Gibson, S. E.; Keen, S. P. Cross-metathesis of unsaturated α -amino acid derivatives. *J. Chem. Soc., Perkin. Trans. 1* **1998**, 2485–2499.
- (41) Oppolzer, W.; Lienard, P. Non-destructive cleavage of N-acylsulfams under neutral conditions: preparation of enantiomerically pure, Fmoc-protected α -amino acids. *Helv. Chim. Acta* **1992**, *75*, 2572–2582.
- (42) Douat, C.; Heitz, A.; Martinez, J.; Fehrentz, J.-A. Stereoselective synthesis of allyl- and homoallylglycines. *Tetrahedron Lett.* **2001**, *42*, 3319–3321.
- (43) Scholl, M.; Ding, S.; Lee, C. W.; Grubbs, R. H. Synthesis and activity of a new generation of ruthenium-based olefin metathesis catalysts coordinated with 1,3-dimesityl-4,5-dihydroimidazol-2-ylidene ligands. *Org. Lett.* **1999**, *1*, 953–956.
- (44) Tamaki, M.; Han, G.; Hruby, V. J. Practical and efficient synthesis of orthogonally protected constrained 4-guanidino prolines. *J. Org. Chem.* **2001**, *66*, 1038–1042.
- (45) Tamamura, H.; Sugioka, M.; Odagaki, Y.; Omagari, A.; Kan, Y.; Oishi, S.; Nakashima, H.; Yamamoto, N.; Peiper, S. C.; Hamanaka, N.; Otaka, A.; Fujii, N. Conformational study of a highly specific CXCR4 inhibitor, T140, disclosing the close proximity of its intrinsic pharmacophores associated with strong anti-HIV activity. *Bioorg. Med. Chem. Lett.* **2001**, *11*, 359–362 and 2409.
- (46) Intramolecular hydrogen bonds were not observed in the calculated structures of these cyclic pentapeptides. Thus, these peptides do not seem to exist in a characteristic turn conformation such as a $\beta III'$ turn as reported in several papers concerning normal cyclic pentapeptides, see Weisshoff, H.; Prasang, C.; Henklein, P.; Frommel, C.; Zschunke, A.; Mugge, C. Mimicry of $\beta III'$ -turns of proteins in cyclic pentapeptides with one and without D-amino acids. *Eur. J. Biochem.* **1999**, *259*, 776–788.
- (47) Murakami, T.; Nakajima, T.; Koyanagi, Y.; Tachibana, K.; Fujii, N.; Tamamura, H.; Yoshida, N.; Waki, M.; Matsumoto, A.; Yoshie, O.; Kishimoto, T.; Yamamoto, N.; Nagasawa, T. A small molecule CXCR4 inhibitor that blocks T cell line-tropic HIV-1 infection. *J. Exp. Med.* **1997**, *186*, 1389–1393.
- (48) Schols, D.; Struyf, S.; Van Damme, J.; Este, J. A.; Henson, G.; De Clercq, E. Inhibition of T-tropic HIV strains by selective antagonization of the chemokine receptor CXCR4. *J. Exp. Med.* **1997**, *186*, 1383–1388.
- (49) Donzella, G. A.; Schols, D.; Lin, S. W.; Este, J. A.; Nagashima, K. A.; Maddon, P. J.; Allaway, G. P.; Sakmar, T. P.; Henson, G.; De Clercq, E.; Moore, J. P. AMD3100, a small molecule inhibitor of HIV-1 entry via the CXCR4 co-receptor. *Nat. Med.* **1998**, *4*, 72–77.
- (50) Doranz, B. J.; Grovit-Ferbas, K.; Sharron, M. P.; Mao, S.-H.; Bidwell Goetz, M.; Daar, E. S.; Doms, R. W.; O'Brien, W. A. A small-molecule inhibitor directed against the chemokine receptor CXCR4 prevents its use as an HIV-1 coreceptor. *J. Exp. Med.* **1997**, *186*, 1395–1400.
- (51) Howard, O. M. Z.; Oppenheim, J. J.; Hollingshead, M. G.; Covey, J. M.; Bigelow, J.; McCormack, J. J.; Buckheit, Jr., R. W.; Clanton, D. J.; Turpin, J. A.; Rice, W. G. Inhibition of in vitro and in vivo HIV replication by a distamycin analogue that interferes with chemokine receptor function: a candidate for chemotherapeutic and microbicidal application. *J. Med. Chem.* **1998**, *41*, 2184–2193.
- (52) Fujii, N.; Nakashima, H.; Tamamura, H. The Therapeutic Potential of CXCR4 Antagonists in the Treatment of HIV. *Expert Opin. Investig. Drugs* **2003**, *12*, 185–195.
- (53) Tamamura, H.; Fujii, N. Two Orthogonal Approaches to Overcome Multi-Drug Resistant HIV-1s: Development of Protease Inhibitors and Entry Inhibitors Based on CXCR4 Antagonists. *Curr. Drug Targets-Infect. Disord.* **2004**, *4*, 103–110.
- (54) Navenot, J. M.; Wang, Z. X.; Trent, J. O.; Murray, J. L.; Hu, Q. X.; DeLeeuw, L.; Moore, P. S.; Chang, Y.; Peiper, S. C. Molecular anatomy of CCR5 engagement by physiologic and viral chemokines and HIV-1 envelope glycoproteins: Differences in primary structural requirements for RANTES, MIP-1 α , and vMIP-II binding. *J. Mol. Biol.* **2001**, *313*, 1181–1193.
- (55) Miyamoto, K.; Nakagawa, T.; Kuroda, Y. Solution structure of the cytoplasmic linker between domain III–S6 and domain IV–S1 (III–IV linker) of the rat brain sodium channel in SDS micelles. *Biopolymers* **2001**, *59*, 380–393.
- (56) Ludvigsen, S.; Andersen, K. V.; Poulsen, F. M. Accurate measurements of coupling-constants from 2-dimensional nuclear-magnetic-resonance spectra of proteins and determination of ϕ -angles. *J. Mol. Biol.* **1991**, *217*, 731–736.

JM050009H

Stereoselective Synthesis of [L-Arg-L/D-3-(2-naphthyl)alanine]-Type (*E*)-Alkene Dipeptide Isosteres and Its Application to the Synthesis and Biological Evaluation of Pseudopeptide Analogues of the CXCR4 Antagonist FC131

Hirokazu Tamamura,^{*,†} Kenichi Hiramatsu,[†] Satoshi Ueda,[‡] Zixuan Wang,[‡] Shuichi Kusano,[§] Shigemi Terakubo,[§] John O. Trent,^{||} Stephen C. Peiper,[‡] Naoki Yamamoto,[†] Hideki Nakashima,[§] Akira Otaka,[†] and Nobutaka Fujii^{*,†}

Graduate School of Pharmaceutical Sciences, Kyoto University, Sakyo-ku, Kyoto 606-8501, Japan, Medical College of Georgia, Augusta, Georgia 30912, St. Marianna University, School of Medicine, Miyamae-ku, Kawasaki 216-8511, Japan, James Graham Brown Cancer Center, University of Louisville, Louisville, Kentucky 40202, and Tokyo Medical and Dental University, School of Medicine, Bunkyo-ku, Tokyo 113-8519, Japan

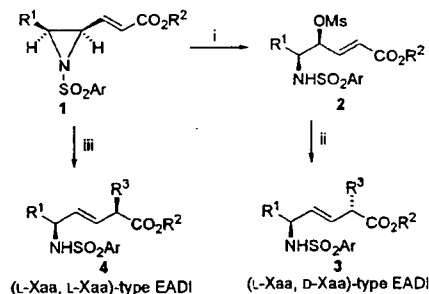
Received July 18, 2004

L,L-Type and L,D-type (*E*)-alkene dipeptide isosteres (EADIs) that have unnatural side chains at the α -position were synthesized by the combination of stereoselective aziridiny ring-opening reactions and organozinc–copper-mediated *anti*-S_N2' reactions toward a single substrate of γ,δ -*cis*- γ,δ -epimino (*E*)- α,β -enoate. The utility of this methodology was demonstrated by the stereoselective synthesis of a set of diastereomeric EADIs of L-Arg-L/D-3-(2-naphthyl)alanine (Nal) that is contained in a small CXCR4 antagonist FC131 [*cyclo*(-D-Tyr-Arg-Arg-Nal-Gly-)]. Furthermore, a (Nal-Gly)-type EADI was synthesized by samarium diiodide (SmI₂)-induced reduction of a γ -acetoxy- α,β -enoate. Several FC131 analogues, in which these EADIs were inserted for reduction of their peptide character, were synthesized with analogues containing reduced amide-type dipeptide isosteres to investigate the importance of these amide bonds for anti-HIV and CXCR4-antagonistic activity.

Introduction

The practical utility of (*E*)-alkene dipeptide isosteres (EADIs) has been intensively investigated in structure–activity relationship (SAR) studies of biologically active peptides toward development of peptide-lead drugs.^{1–7} Backbone replacements of amide bonds in peptides by EADIs provide information on the contributions of the corresponding amide bonds on biological activity. We previously established a completely stereocontrolled synthetic process for L,L-type and L,D-type EADIs starting from L-amino acid.^{8,9} As shown in Scheme 1, treatment of *N*-aryl- γ,δ -*cis*- γ,δ -epimino (*E*)- α,β -enoates (*cis*-(*E*)-enoates) **1** with methanesulfonic acid (MSA) gives γ -mesyloxy- α,β -enoates **2**, which can be converted into L,D-type EADIs **3** by organocopper-mediated α -alkylation via *anti*-S_N2' reactions, whereas organocopper treatment of *cis*-(*E*)-enoates **1** affords L,L-type EADIs **4**. However, this synthetic procedure has not yet been optimized, because it involves a potential limitation on the introduction of functional groups into the side chain (R³) at the α -position. In a standard procedure, organocopper reagents, which were prepared by CuCN and RLi or RMgX (X = Cl or Br), are used for α -alkylation.^{2,4} In the α -alkylation of the synthesis of (Xaa-L/D-Glu)-type EADIs,¹⁰ organozinc–copper reagents are used, which are prepared from IZnCH₂CH₂CO₂R and

Scheme 1^a



^a R¹, R², R³ = alkyl; Ar = 2,4,6-trimethylphenylsulfonyl (Mts) or Ts. Reagents: (i) MsOH; (ii) R³Cu(CN)MgX·BF₃ (X = Cl or Br) or R³Cu(CN)Li·BF₃; (iii) R³Cu(CN)MgX·2LiX (X = Cl or Br) or R³Cu(CN)Li·2LiX.

CuCN.^{11–15} In this study, to demonstrate the general utility of organozinc–copper reagents, a set of EADIs of L-Arg-L/D-3-(2-naphthyl)alanine (Nal) were synthesized as model compounds via the γ,δ -*cis*- γ,δ -epimino (*E*)- α,β -enoate by the combination of MSA-mediated aziridiny ring-opening reactions and α -alkylation with organozinc–copper reagents, which were prepared from 2-naphthylmethylZnBr and CuCN. The dipeptide sequence, Arg-Nal, is part of the low molecular weight CXCR4 antagonist, FC131, which was recently developed by us (Figure 1).¹⁶

CXCR4 is a chemokine receptor, which is involved in cell progression and metastasis of several types of cancer,^{17–19} HIV entry,²⁰ and rheumatoid arthritis.^{21,22} Thus, several inhibitors directed against CXCR4 have been developed.^{23–27} We previously found a highly potent CXCR4 antagonist, T140, which is a 14-mer

* Corresponding authors. Tel: +81 75 753 4551, Fax: +81 75 753 4570, E-mail: tamamura@pharm.kyoto-u.ac.jp; nfujii@pharm.kyoto-u.ac.jp.

[†] Kyoto University.

[‡] Medical College of Georgia.

[§] St. Marianna University.

^{||} University of Louisville.

[‡] Tokyo Medical and Dental University.